Compaction and sintering of Hydroxyapatite

A Thesis submitted to Department of Materials Engineering, School of Chemical and Materials Engineering (SCME), NUST, in partial fulfillment of the requirements for the degree of

MASTER OF SCIENCE (MS)
In
MATERIALS AND SURFACE ENGINEERING

By
MUHAMMAD YASIR
2009-NUST-MS Ph.D-MS-E-09

Supervised By
Dr. MOHAMMAD MUJAHID

SCHOOL OF CHEMICAL AND MATERIALS ENGINEERING (SCME),
NATIONAL UNIVERSITY OF SCIENCESAND TECHNOLOGY (NUST),
H-12, ISLAMABAD, PAKISTAN,
2011.

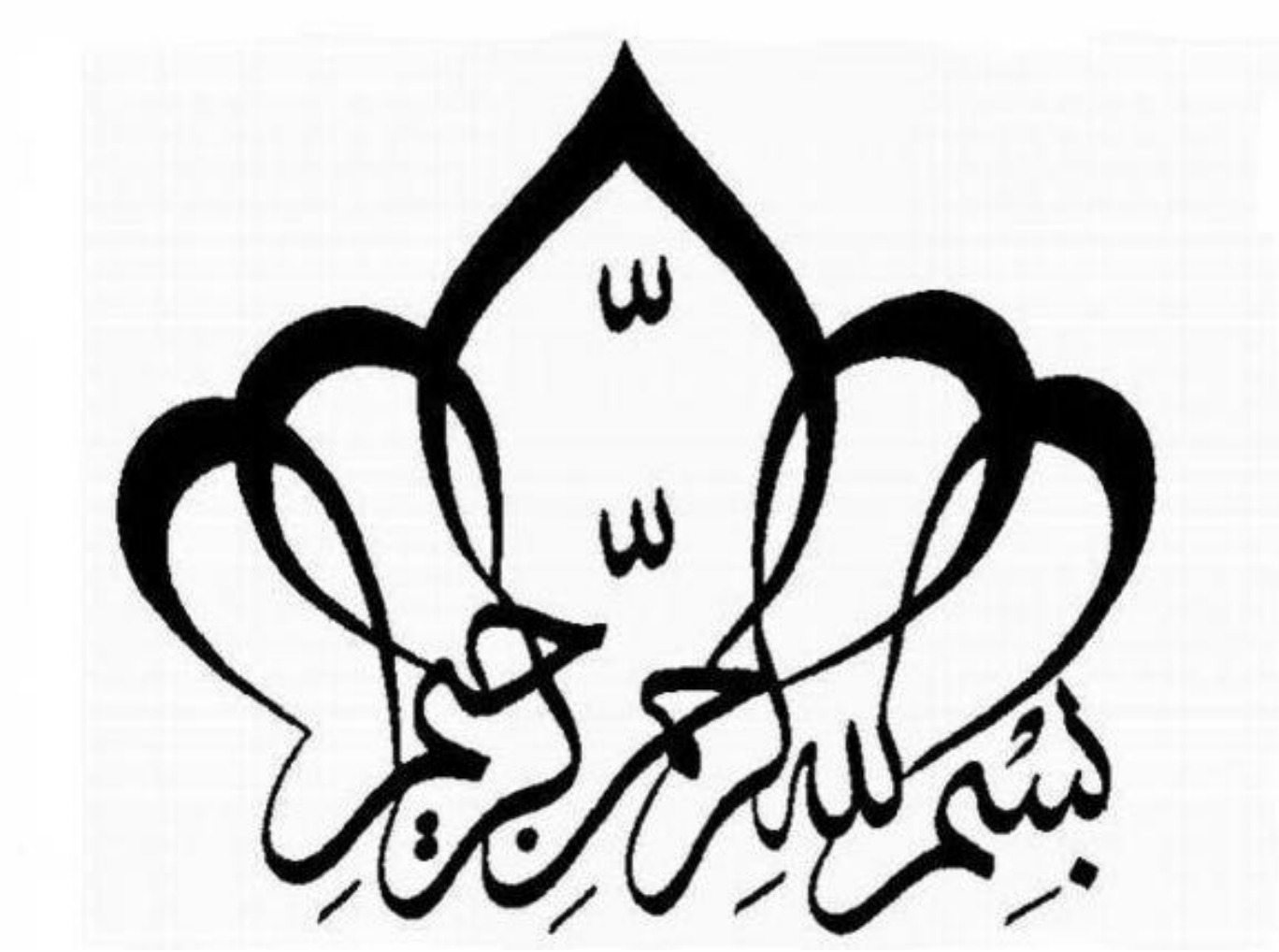
بسم الله الرحمن الرحيم

CERTIFICATE

This is to certify that the work in this dissertation has been carried out by Muhammad Yasir and completed under my supervision at School of Chemical and Materials Engineering, National University of Science and Technology, Islamabad, Pakistan.

Dr. Mohammad Mujahid

Supervisor
School of Chemical and Materials Engineering,
National University of Science and Technology,
Islamabad, Pakistan.

Submitted through

Prof. Dr. Mohammad Shahid

Head of Department
School of Chemical and Materials Engineering,
National University of Science and Technology,
Islamabad, Pakistan.

ACKNOWLEDGEMENT

All praise to Almighty Allah, the Lord of all the worlds. It is undeniable that all manifestation of nature bears eloquent testimony to the fact that Allah is the Creator, the Maintainer and the Regulator of the world. He makes Laws for the evaluations of things and sets them on the path of perfection. Almighty Allah who bestows and blesses knowledge, technology and scientific ingenuity to man through experimental research and remarkable deduction to ponder over the forces of nature. In the first place, therefore, I express my utmost thanks to Almighty Allah the Omnipresent and the Creator of the worlds, Who has endowed us brain and instable instinct construction of knowledge and body to accomplish our work in the form of this project report.

"No doubt, appreciation is prior to acknowledgement; quality of the latter is superior to the essence of the former."

I offer my gratitude to the last Prophet MUHAMMAD (S.A.W), who has given the lesson of LOVE, HUMANITY, PARITY, and JUSTICE and also broke the cage of servitude through His golden sayings, to seek knowledge is obligatory for every Muslims.

The saying of the Prophet (S.A.W.)

"Acquire knowledge even if you have to go to china." tells the importance of knowledge.

I express my sincere thanks to my respected supervisor Dr. Mohammad Mujahid for his worthy guidance in his kind supervision on all the practical work performed. I have always looked up to him for guidance in any problem I faced in my work and I consider myself privileged to work under his supervision.

It is my pleasure to appreciate and thank Dr. Mohammad Islam, my Co-supervisor for his inspiring way of teaching and guiding. I am thankful to Dr. Mohammad Mazhar from PIEAS who helped me in conducting flexural strength experiments at PIEAS and fruitful guidance for my research work. I feel honor to acknowledge Dr. Arshad Head of Chemical Engineering Department for providing the laboratory facilities. I would also like to thank all the faculty members, non-teaching staff and my fellow students for the help provided to me at the various stages.

My deep appreciation and a bundle of thanks for Prof. Dr. Mohammad Shahid Head of materials engineering department, SCME for his sincere and inspiring guidance.

I acknowledge School of Chemical and Materials Engineering (SCME), NUST, Pakistan, for the technical and financial assistance provided during my research.

Last but not the least I will like to thank my Parents, without their confidence in me and support this work would have never been accomplished.

Muhammad Yasir

DEDICATION

I Dedicate My Thesis to My Parents, Supervisor and Instructors Who Inspired Me to Higher Ideas of Life and Taught the Ups and Downs of Life.

Abstract

The effect of compaction load, sintering temperature and soaking time on the sinterability and densification of Nanocrystalline hydroxyapatite (HA) was assessed in this work. The compaction and sinterability of Nanocrystalline hydroxyapatite (HA) particles was done at three different compaction loads and temperatures ranging from 1 ton to 5 ton and 850^0C to 1250^0C respectively. Green and sintered densities of the compacts were analyzed by Archimedes method (for density measurements) for the influence of these parameters. The results revealed that compaction of the green pellets was best achieved at 5 ton compaction load and its percent green densification was up to 50% of the theoretical density of HA ($3.16 g/cm^3$). For sintered density, the best results were achieved at a temperature of 1250^0C and a compaction load of 1 ton which were 98% of the theoretical density. Soaking time at these sintering temperatures was varied between 1 and 3 hours and was found that with the variation of soaking time from 3 hours to 1 hour, the sintered density decreased tremendously at 850^0C from 85% to 50% whereas at higher temperatures the decrease in density was only 4 to 6%. Vickers micro hardness testing and biaxial flexural testing was used to evaluate hardness and flexural strength of sintered compacts respectively. The maximum hardness of 625 ($\pm$28) HV1 and flexural strength of 40 ($\pm$10) MPa was obtained for HA sintered at 1250^0C with a soaking time of 3 hours. Phase analyses were carried out using an X-Ray diffractometer. The HA phase was stable even at the highest sintering temperature of 1250^0C and did not decompose into α tri-calcium phosphate (TCP) and β TCP.

Table of Contents

List of Figures

List of Tables

Chapter 1

Introduction

Introduction 1

1.1 Background

The increasing need to revolutionize the modern treatment and bio-implants has prompted a wave of research into the field of biomaterials. Bio-ceramics is one of the latest and primary implants for bone substitute materials in modern health care industries due to their low density, chemical stability, high wear resistance and compositional similarities with human bone [1]. While the potential of any ceramic material to be used as an implant is based upon its strength and bio-compatibility with host environment.

Few bio-material scientists focus on the fabrication and enhancement of bioactive capabilities of calcium phosphate and in particular much interest has been directed towards the use of hydroxyapatite (HA).

The first officially reported medical application of calcium phosphate bio-ceramic in human body was in 1920 [2]. In 1975 the dental applications were also reported [2]. Calcium phosphate biomaterials are frequently used in the repair of the dental and musculoskeletal systems. Hydroxyapatite has been used as a coating for dental applications such as tooth implants. For musculoskeletal systems, calcium phosphate has various significant roles from spinal fusions to the replacement of minor load bearing joints.

Calcium phosphate exists in different phases depending on temperature, impurities and the presence of water [2]. Different phases of calcium phosphate ceramics are used by the modern health care industry, depending upon whether a reasonable or bio active material is desired [2]. Two phases that are stable at body temperature and in contact with body fluid are di-calcium phosphate ($CaHPO_4^{-2}H_2O$)vat pH below 4.2 and hydroxyapatite (HA) ($Ca_{10}(PO_4)_6(OH)_2$) at pH above 4.2. Human blood stays in a very narrow pH range ≈ 7.3. Clearly, HA is a stable phase in that pH and also the ideal phase for applications inside human body.

Hydroxyapatite material has been clinically applied in many areas of dentistry and orthopedics because of its excellent osteoconductive and bioactive properties which is due to its chemical similarity with the mineral portion of hard tissues [3].

It appears to form a direct chemical bond with hard tissues. Substitution of OH^- with F^- gives the apatite greater chemical stability due to the closer coordination of fluoride as compared to the hydroxyl by the nearest calcium [3]. Despite chemical similarities of synthetic HA to the mineral phase of bone, it differs significantly in mechanical and biological properties of that of natural bone.

HA has poor mechanical properties, which has so far restricted their use to non-load bearing applications such as coatings. One of the major concern with HA is the low fracture toughness, i.e. $<1MPam^{1/2}$ of the sintered body [4]. One of the critical controlling parameter that requires attention during the processing of hydroxyapatite is the selection of a suitable sintering method to obtain a solid, high density HA body that is characterized by having fine-grained microstructure.

The poor mechanical properties of HA has so far restricted its use to non-load bearing applications such as coatings. Significant research has focused on enhancing the mechanical abilities of synthetic HA. The challenge to improve the mechanical properties of HA to be used under load bearing applications is one of the major objectives of this research. The sintering of synthetic HA under different compaction loads and sintering temperatures will be done to study the densification and other mechanical properties.

1.2 Objectives

The aim of this research is to achieve following goals:

1) Investigate the effects of different compaction loads on the green density and sintered density of Nanocrystalline HA.
2) To study the effect of different sintering temperatures on the densification and mechanical properties of HA.
3) Observe the effect of different sintering time (soaking time) during sintering on the sintered density of HA.
4) Observe the variation of hardness and flexural strength by increasing sintering temperature.

1.3 Outline

Chapter 1 of the thesis provides an overview and touches the motivations behind this research. Chapter 2 provides an introduction to the biomaterials, in particular hydroxyapatite and its properties as compared to bone. Chapter 3 discusses an overview of compaction and sintering of ceramics affecting the final properties. Chapter 4presents the experimental methodsused anddiscusses the characterization techniques used. Chapter 5 provides a linked discussion of all the results. Chapter 6 presents the conclusions and frame work.

Chapter 4 is divided into sections corresponding to each characterization technique applied to samples: X-ray diffraction, scanning electron microscopy, FTIR spectroscopy, Thermo-gravimetric analysis and Vickers hardness testing

References:

1. Wang, P.E. and Chaki T.K., 1993, Sintering behavior and mechanical properties of hydroxyapatite and di-calcium phosphate, J. Material Science: Mat. Med., pages 150-158
2. Van Landyut, P. Li. F., Keustermans J.P., Sterydio J.M., 1995, The influence of high sintering on the mechanical properties of hydroxyapatite, J. Material Science: Mat. Med., pages 6,8-13
3. Irita I.H., Castano V.M., Wilkinson D.S, 1995, Synthesis and processing of hydroxyapatite tapes with controlled porosity, J. Material Science: Mat. Med., pages 19-23
4. Zhou J., Zhang X., Chen J., Zeng S., D. Groot K., 1993, High temperature of characteristics of hydroxyapatite, J. Material Science: Mat. Med., pages 83-85

Chapter 2 Introduction to Biomaterials

Chapter 2 Introduction to Biomaterials

2.1 Biomaterial

A biomaterial is any material that is designed to interact with biological environment and developed such that to maintain the environment as it is. Biomaterials have been developed for fifty years from now and have led to an extraordinary solution for many biological problems such as implants, joints, supports, bio catalyst, Nano-material medicines etc. Biomaterial science has experienced a steady and strong growth over its history with a lot of new developments and enhancements. Biomaterial covers the aspects of medicine, biology, chemistry, tissue engineering and materials science.

Some earlier biomaterials had applications such as Phoenicia where loose teeth were bound together with gold wires for tying artificial ones to the neighboring teeth. In early 1900's first experiment of implantation of plates for bones was done successfully which assisted the bone fractures providing them protection as they heal. In 1950's to 60's, blood vessels were also artificially replaced for the cancerous and defected ones [1]. Then heart surgery and valve replacement was practiced and is still being developed for betterment.

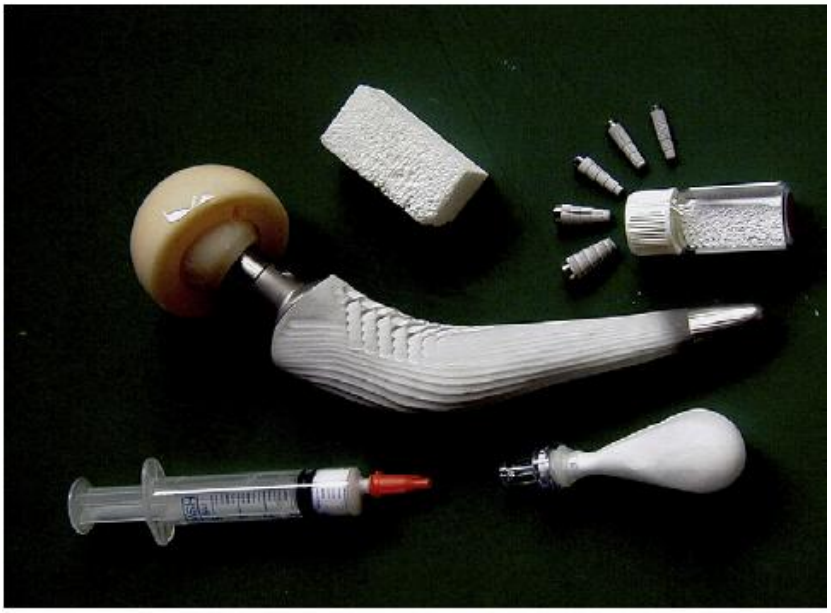

Figure 2.1 several examples of commercial calcium orthophosphate-based bio-ceramics[1]

A bio-ceramic is defined as a ceramic used as a biomaterial. The field of bio-ceramics is relatively new; it did not exist until the 1970s.Bio-ceramics are implanted into the human body to replace existing parts that have become diseased, damaged, or worn out. More than 1 million hip prostheses using aluminacomponents have been performed. Alumina is a very important bio-ceramic because it is biocompatible;it does not produce any adverse reactions in the body. One of the disadvantages of alumina is that it is also an example of what is termed a nearly inert bio-ceramic: it does not allow interfacial bonding with tissue. When bioactive ceramics and glasses are implanted into the body they undergo chemical reactions on their surface leading to strong bond formation. The most important bioactive ceramic is hydroxyapatite (HA), which is very similar to the mineral part of teeth and bones. HA is brittle and mechanically weak, but if it is combined with a polymer a composite can be produced that is ductile and has E close to that of bone. HA and other bioactive ceramics and glasses are often used as coatings on metal supports. This allows the excellent mechanical properties of the metal to be combined with the biocompatibility of ceramics. Another ceramic material that is used in the form of a coating is pyro-lytic carbon. The application here is artificial heart valves, which is a very demanding materials application: reliability is critical.

Table 2.1 Classification scheme for Bioceramics[7]

Classification scheme for Bio-ceramics
Nearly inert bio-ceramics
Examples: Al2O3, low-temperature isotropic (LTI) carbon; ultraLTI carbon; vitreous carbon; ZrO2
Tissue attachment: Mechanical
Bioactive ceramics
Examples: HA; bioactive glasses; bioactive glass-ceramics
Tissue attachment: Interfacial bonding
Resorbable bio-ceramics
Examples: Tri-calcium phosphate (TCP); calcium sulfate; trisodium phosphate
Tissue attachment: Replacement
Composites
Examples: HA/auto-genius bone; surface-active glass ceramics/ polymethyl methacrylate (PMMA); surface-active glass/ metal fibers; poly-lactic acid (PLA)/carbon fibers; PLA/HA;PLA/calcium/phosphorus-based glass fi bers
Tissue attachment: Depends on materials

If it is possible to introduce a practically most possible inert material into a body, it initiates a protective response that leads to encapsulation through a non-adherent fibrous coating about 1 μm thick. As times, this phenomenon leads to total isolation of the implant. A similar response is reported when a similarly featured metallic or polymeric material is introduced. While bio-active ceramics has different behavior and as a result, the body responds the implant as a natural part and reacts in the natural repair response. Bio-active ceramics such as HA may be used in bulk form or as a part of a composite or as a coating. Resorbable bio-ceramics, such as tricalcium phosphate (TCP), actually dissolve in the body and are replaced by the surrounding tissue.

It is an important requirement, of course, that the dissolution products are not toxic. As in the case of HA, TCP is often used as a coating rather than in bulk form. It is also used in powder form, e.g., for filling space in bone. Figure 2.2 shows a number of clinical uses of bioceramics. The uses go from head to toe and include repairs to bones, joints, and teeth.

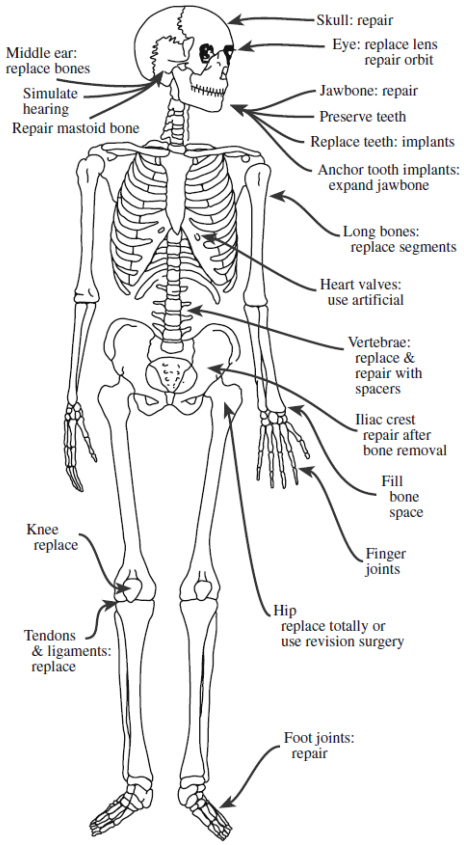

Figure 2.2 Illustration of the head-to-toe clinical uses for bioceramics[2]

These implants are very significant where the cases lay in the boundary of being diseased, damaged or just simply worn out. There are many other applications of bioceramics including

pyrolytic carbon coatings for heart valves and special radioactive glass formulations for treatment of particular tumors.

2.2 Performance Assessment of Biomaterials [3]

The success of biomaterials in the body depends on factors such as the material properties, design, and biocompatibility of the material used, as well as other factors not under the control of the engineer, including the technique used by the surgeon, the health and condition of the patient, and the activities of the patient. If we can assign a numerical value f to the probability of failure of an implant, then the reliability can be expressed as

$R = 1 - f$

If, as is usually the case, there are multiple modes of failure, the total reliability rt is given by the product of the individual reliabilities r1 = (1-f1), etc.

$Rt = r1 \times r2 \times \ldots.. rn$

Consequently, even if one failure mode such as implant fracture is perfectly controlled so that the corresponding reliability is unity, other failure modes such as infection could severely limit the utility represented by the total reliability of the implant. One mode of failure which can occur in a biomaterial, but not in engineering materials used in other contexts, is an attack by the body's immune system on the implant. Another such failure mode is an unwanted effect of the implant upon the body; for example, toxicity, inducing allergic reactions, or causing cancer. Consequently, biocompatibility is included as a material requirement in addition to those requirements associated directly with the function of the implant. Biocompatibility involves the acceptance of an artificial implant by the surrounding tissues and by the body as a whole. Biocompatible materials do not irritate the surrounding structures, do not provoke an abnormal inflammatory response, do not incite allergic or immunologic reactions, and do not cause cancer. Other compatibility characteristics which may be important in the function of an implant device made of biomaterials include (1) adequate mechanical properties such as strength, stiffness, and fatigue properties; (2) appropriate optical properties if the material is to be used in the eye, skin, or tooth; and (3) appropriate density. Sterilizability, manufacturability, long-term storage, and appropriate engineering design are also to be considered. The failure modes may differ in importance as time passes following the implant surgery. For example, consider the case of a

total joint replacement in which infection is most likely soon after surgery, while loosening and implant fracture become progressively more important as time goes on. Failure modes also depend on the type of implant and its location and function in the body. For example, an artificial blood vessel is more likely to cause problems by inducing a clot or becoming clogged with thrombus than by breaking or tearing mechanically.

2.3Types of Biomaterials

In the selection of a material for a particular application we always have a choice. Materials selection is a critical part of any component design process and is especially important for implants and other medical devices. The three main classes of material from which we can select for a load-bearing application are metals, polymers, and ceramics. Table 2.3 is a comparative list of the significant physical properties of different biomaterials from each of the three classical material classes. Table 2.2 compares the behavior of these different classes relevant to their potential use as implants.

Material class	*Advantages*	*Disadvantages*
Polymer	Resilient	Weak
	Tough	Low modulus value
	Easy to fabricate	Not usually bio-active
	Low density	Not resorbable
Metal	Strong	Can corrode
	Wear resistant	High value of modulus
	Tough	High density
	Easy to fabricate	Not usually bio-active
		Not resobable
Ceramic	Bio-compatible	Low tensile strength
	Wear resistant	Low toughness
	Certain composition are also light weight	Difficult to fabricate
		Not resilient

TABLE 2.2 General Comparisons of Materials for Implants [6]

2.3.1 Significant properties of Biomaterials

The main advantage of ceramics over other implant materials is their biocompatibility: some are inert in the physiological environment while others have a controlled reaction in the body. The main disadvantages of most bioceramics are

- Low toughness (which can affect reliability)
- High E (which can lead to stress shielding)

One of the main ways of increasing the toughness of ceramics is to form a composite. The ceramic may be the reinforcement phase, the matrix, or both. An example of a polymer−matrix composite (PMC) reinforced with a bioceramic is polyethylene (PE) reinforced with HA particles. The toughness of the composite is greater than that of HA and E is more closely matched to that of bone.

Material	Density (g/cm^3)	UTS (Mpa)	Compressive strength (Mpa)	Modulus 'E' (GPa)	K_{1C} ($MPa\ m^{1/2}$)	Hardness (knoop)	a (ppm^2C)	Fracture surface energy (J/m^2)	Poisson's ratio	k ($Wm^{-1}K^{-1}$)
HA	3.1	40-300	300-900	80-120	0.6-1.0	400-4500	1.1	2.3-2.0	0.28	
TCP	3.14	40-120	450-650	90-120	1.2		14-15	6.3-8.1		1.5-3.6
Bioglasses	1.8-2.9	20-350	800-1200	40-120	2	4000-5000	8-14	14-50	0.21-0.24	
SiO_2 glass	2.2	70-120		70	0.7-0.8	7000-7500	0.6	3.5-4.6	0.17	1.5
Al_2O_3	3.85-3.99	270-500	3000-5000	380-410	3-6	15000-20000	6-9	7.6-30	0.27	30
PSZ	5.6-5.89	500-650	1850	195-210	5-8	17000	9.8	160-350	0.27	4.11
Si_2N_4	3.18	600-850	500-2500	300-320	3.5-8.0	22000	3.2	20-100	0.27	10-25
SiC	3.10-3.21	250-600	650	350-450	3-6	27000	4.3-5.5	22-40	0.27	100-150
Graphite	1.5-2.25	5.6-25	35-360	3.5-12	1.9-3.5		1-3	500	0.3	120-180
Carbon fibre	1.5-1.8	400-5000	330-360	250-700						
Glassy carbon	1.4-1.6	150-250	600	2.5-40		8200	2.3-3.2			
PE	0.9-1.0	0.5-65		0.1-1.0	0.4-4.0	170	11-22	500-8000	0.4	0.3-6.5
PMMA	1.2	60-70	80	3.5	1.5	160	5-8.81	300-400		
Ti	4.52	345	250-600	117	60	1800-2600	8.7-10.1	15000	0.31	
Ti/Al/V alloys	4.4	780-1050	450-1850	110	40-70	3200-3600	8.7-9.5	10000	0.34	
Vitalium alloys	7.8-8.2	400-1030	48-600	230	120-160	3000	15.6-17.0	5000	0.3	
Low C alloys	7.8-8.2	540-4000	1000-4000	200	55-95	1200-9000	16-19	50000	0.2-0.33	4.6

TABLE 2.3 Significant Physical Properties of different bio-materials[1]

2.4 STRUCTURE OF BONE

Bone is a living material composed of cells and a blood supply encased in a strong composite structure. The composite consists of collagen, which is flexible and very tough, and crystals of an ‘apatite’ of calcium and phosphate, resembling calcium hydroxyapatite; we will proceed as if it is HA. It is the HA component that gives bone its hardness. The acicular apatite crystals are 20–40 nm in length and 1.5–3 nm wide in the collagen fiber matrix. Two of the various types of bone that are of most concern in the use of bioceramics are

- Cancellous (spongy bone)
- Cortical (compact bone)

Cancellous bone is less dense than cortical bone. Every bone of the skeleton has a dense outer layer of compact bone covering the spongy bone, which is in the form of a honeycomb of small needle-like or flat pieces called trabeculae. Figure 2.2 is a schematic showing a longitudinal section of a long bone.

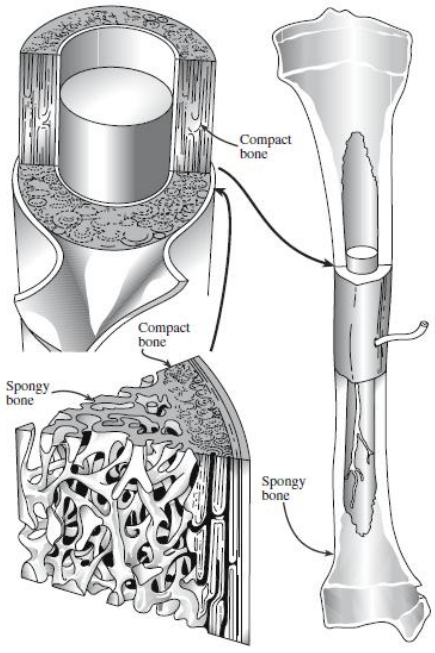

Figure 2.3 Longitudinal sectionshowing the structure oflong bone [5]

The open spaces between the trabeculae are filled with red or yellow bone marrow in living bones. Because of its lower density, cancellous bone has a lower E and higher strain-to-failure ratio than cortical bone, as shown in Table 2.4.

TABLE 2.4 Mechanical Properties of Skeletal Tissues[5]

Property	Cortical bone	Cancellous bone	Articular cartilage	Tendon
Compressive strength (Mpa)	100*230	2-12		
Flexural strength (MPa)	50-150	10-20	10-40	80-120
Strain to failure	1-3%	5-7%	15-50%	10%
Modulus 'E' (GPa)	7-30	0.05-0.5	0.001-0.01	1
K_{1C} (Mpa $m^{1/2}$)	2-12			
Compressive stiffness (N/mm)			20-60	
Compessive creep modulus (MPa)			4-15	
Tensile stiffness (Mpa)			50-225	

Both types of bone have higher E than soft connective tissues, such as tendons and ligaments. The difference in E between the various types of connective tissues ensures a smooth gradient in mechanical stress across a bone, between bones, and between muscles and bones.

2.4.1 BONE MATRIX

The bone matrix is composed of:

- Organic matter
- Inorganic matter

2.4.1.1 Organic matter

Organic matter consists of type I collagen fibres embedded in the ground substance containing proteoglycans and glycoproteins. The collagen fibres are made up of bundles of fibrils to resist pulling forces.

2.4.1.2 Inorganic matter

Inorganic matter is made up of stiffening substances to resist bending and compression. The bone mineral is an analogue of crystals of calcium phosphate hydroxyapatite

$Ca_{10}(PO_4)_6(OH)_2$ (HA). It is this association of hydroxyapatite with collagen fibres which is responsible for the hardness of bone.

2.5 Hydroxyapatite

Synthetic hydroxyapatite is similar in composition to the mineral component of bone and teeth. This similarity has led to interest in the development of HA materials for biomedical applications. The table below[8] illustrates the chemical and structural similarities between HA, enamel, dentin, and bone.

Table 2.5 Chemical and structural comparison of teeth, bone, and HA[8]

Composition,wt%	**Enamel**	**Dentin**	**Bone**	**HA**
Calcium	36.5	35.1	34.8	39.6
Phosphorus	17.1	16.9	15.2	18.5
Ca/P ratio	1.63	1.61	1.71	1.67
Total inorganic (%)	97	70	65	100
Total organic (%)	1.5	20	25	--
Water (%)	1.5	10	10	--
Crystallographic properties: Lattice parameters (± 0.003Å)				
a-axis (Å)	9.441	9.421	9.41	9.430
c-axis (Å)	6.880	6.887	6.89	6.891
Crystallinity index, (HA=100)	7.-75	33-37	33-37	100

Crystallographically, hydroxyapatite belongs to the hexagonal system with the P63/m space group. The 'P' indicates that HA is a primitive hexagonal system where a = b ≠ c, α=β=90° and γ=60°[9]. A schematic representation of the crystal structure is provided in Figure 2.4.[10]

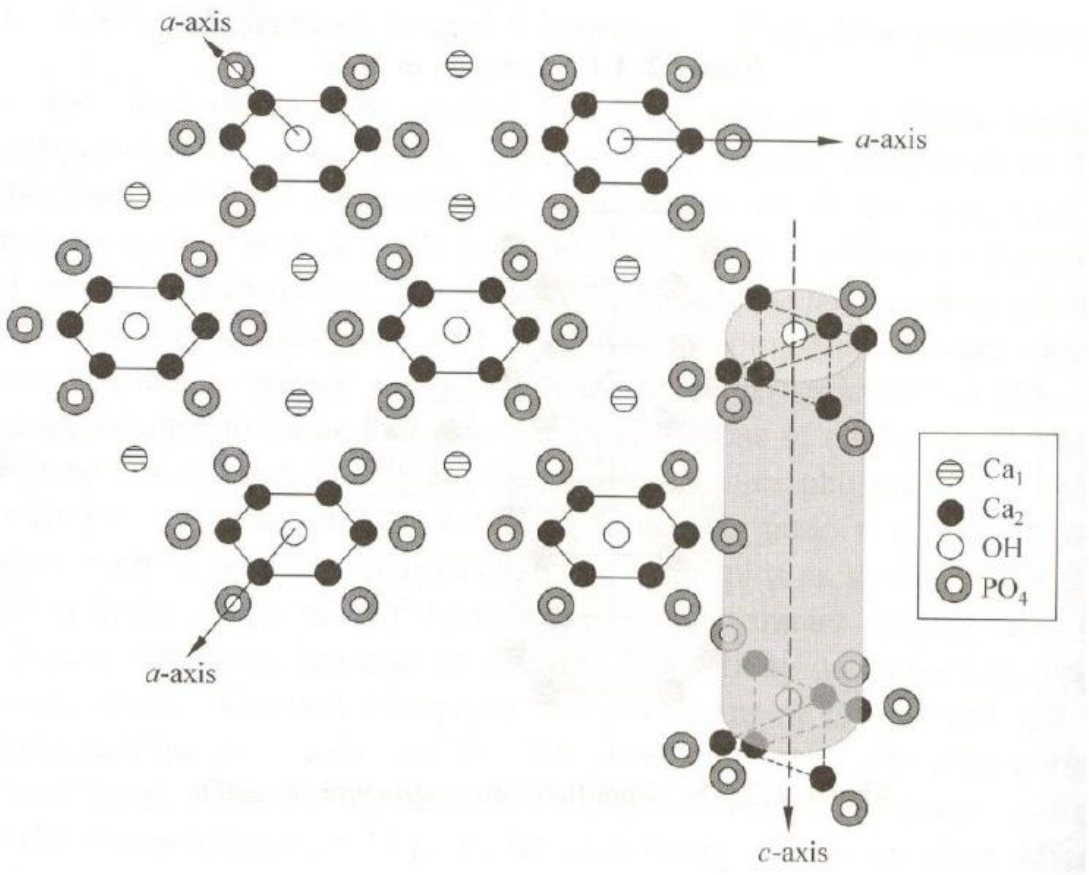

Figure 2.4 Schematic representation of hydroxyapatite crystal structure. [10]

According tostoichiometry the ideal atomic ratio of Ca to P is 1.67[8]. HA have density value of 3.16g/cm3. Depending upon the synthesis process, conditions,morphology and structure HAhave wide range of mechanical properties.These properties arecomparable with the natural composites like bone and dentine. Dental enamel havingelastic modulus of 74 GPa is the stiffest hard tissue because it contains most mineral,while dentine and compact bone have low elastic modulus of 21 GPa and 18 GPa due to less percentage of mineral phase. Poisson ratio of HA is 0.27 very close to that of Bone 0.3[11].

Hydroxyapatite is biocompatible and bioactive as it appears to form a direct chemicalbond with hard tissues of the body [12] after implantation of hydroxyapatite particles orporous blocksinbone, new lamellar cancellous bone forms within 4 to 8 weeks [13].

References:

1. Lemon JE., 1996, Ceramics: past, present and future. Bone, section 19(1 Suppl.), pages 12–85
2. Ducheyne P, Qiu Q., 1990, Bioactive ceramics: the effect of surface reactivity on bone formation and bone cell function Biomaterials, section 2, pages 287–303
3. Black, J. (1992) Biological Performance of Materials, 2nd ed. (New York: Marcel
4. Dekker).Irita I.H., Castano V.M., Wilkinson D.S, 1995, Synthesis and processing of hydroxyapatite tapes with controlled porosity, J. Material Science: Mat. Med., pages 19-23
5. Zhou J., Zhang X., Chen J., Zeng S., D. Groot K., 1993, High temperature of characteristics of hydroxyapatite, J. Material Science: Mat. Med., pages 83-85
6. Ravaglioli A, Krajewski A., 1992, Bioceramics: materials, properties, application., London: Chapman & Hall, p. 156–197
7. Billotte WG, Brozino JD., 2000,The biomedical engineering handbook. 2nd ed., Boca Raton, FL: CRC Press, London: IEEE Press, section 38, pages. 7–18
8. Dorozhkin SV. Calcium orthophosphates. J. Mater. Sci. 42: 1061-1095. 2007.
9. Kay MI, Young RA and Posner AS. Crystal Structure of Hydroxyapatite. Nature 204: 1050-1052. 1964.
10. Shi, Donglu. Introduction to Biomaterials. Tsinghua University Press. 2006.
11. Joon B. Park, Joseph D. Bronzino, Biomaterials; Principles and Applications, CRCPress
12. Piattelli A and Trisi P, A light and laser scanning microscopy study ofbone/hydroxyapatite-coated titanium implants interface: histochemical evidence ofunmineralized material in humans, J. Biomed. Mater 1994
13. Bajpai PK and Fuchs CM. Development of a hydroxyapatite bone grout. In: Proceedings of the First Annual Scientific Session of the Academy of Surgical Research, San Antonio, TX, CW Hall, Ed., pp. 50–54. Pergamon Press, New York 1985
14. Wang, P.E. and Chaki T.K., 1993, Sintering behavior and mechanical properties of hydroxyapatite and di-calcium phosphate, J. Material Science: Mat. Med., pages 150-158
15. Van Landyut, P. Li. F., Keustermans J.P., Sterydio J.M., 1995, The influence of high sintering on the mechanical properties of hydroxyapatite, J. Material Science: Mat. Med., pages 6,8-13
16. Irita I.H., Castano V.M., Wilkinson D.S, 1995, Synthesis and processing of hydroxyapatite tapes with controlled porosity, J. Material Science: Mat. Med., pages 19-23
17. Zhou J., Zhang X., Chen J., Zeng S., D. Groot K., 1993, High temperature of characteristics of hydroxyapatite, J. Material Science: Mat. Med., pages 83-85

Chapter 3 Literature Review on Sintering

Chapter 3 Literature Review on Sintering

3.1 Introduction

In this chapter an effort has been made to cover the route by which Hydroxyapatite was synthesized, some of the general methods of powder compaction and concepts regarding the sintering and its mechanisms along with different stages and factors involved in solid state sintering. Hydroxyapatite was sintered by solid state sintering so a detail literature survey of solid state sintering has been discussed.

3.2 Synthesis of Hydroxyapatite

HA was synthesized by AmTech laboratories and was used in as received condition. The brief method for the synthesis is described here.

The flow chart for the preparation of HA is illustrated in figure below. The materials used in this work included calcium chloride ($CaCl_2$), di-potassium hydrogen phosphate (K_2HPO_4), NaOH and CetylTrimethyl Ammonium Bromide (CTAB). All chemicals were of analytical grade from Merck and aqueous solutions were prepared by dissolving the required amounts in doubly distilled de-ionized water.

Solutions of calcium chloride (1M) and di-potassium hydrogen phosphate (0.6M) were prepared by dissolving the required amounts in 60 ml and 100 ml of de-ionized water respectively. The surfactant solutions, with concentrations ranging from 0.01M to 0.06 M, were prepared by dissolving the required amounts of CTAB in 100 ml of de-ionized water. Both the surfactant and phosphate solutions were added into 100 ml of de-ionized water and the pH of the resulting solution was adjusted at 12 using NaOH. The above solution was kept for two hours to ensure that the cooperative interaction and self-assembly process has been completed.

Subsequently the $CaCl_2$ was slowly added drop-wise to the solution mixture, yielding a milky suspension, which was refluxed at 120°C for 24 hours. The precipitates were then filtered off and washed with de-ionized water. A gel like paste was produced which was then dried in an oven at 100°C for 24 hours. The powder was then calcined in air in a furnace at 550°C for 5 hrs to yield HA powder.

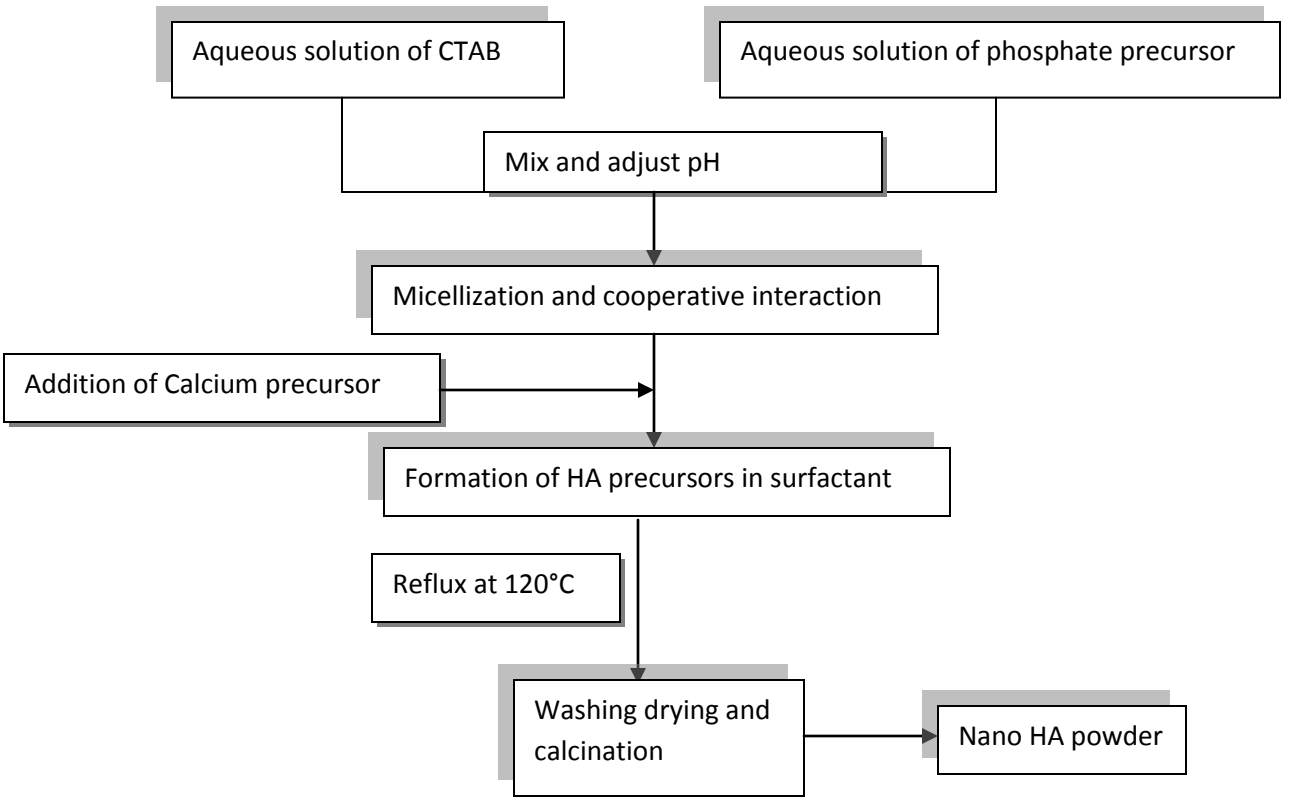

Figure 3.1 Procedure for the synthesis of HA using CTAB[13]

3.3 Powder Processing

The powder is compacted into the desired shape using one of a number of techniques described below. This porous shape, known as a green body, is then densified by heating to a suitable temperature, sometimes with the simultaneous application of pressure.

The mechanical properties of the final product (after sintering) depend critically on the homogeneity of the compact. If a compact contains a range of densities, each region will contract to a different extent on sintering. This means that not only will it have different mechanical properties in different regions but even more important the product will contain internal stresses. This causes problems in both metals and ceramics.

Design of the die/punch is very important. Friction between the powder and the die can lead to a non-uniform density distribution which results in strength variation.

More uniform distribution is achieved by

- better lubrication between powder and die
- Multiple punches, e.g. with punches moving at both top and bottom of die. Get highest compaction close to moving punch, so average compaction increased and compaction variation is reduced.

3.4 Methods of powder compaction

3.4.1 Die pressing

This is by far the most common process for small components with very simple shapes and where very high production rates are required. Because the pressure is not uniformly applied throughout the body, due to frictional effects at the die walls, the final density of the finished part may not be completely uniform.

3.4.2 Iso-static pressing

Powder is put into a flexible rubber mold and then hydrostatically compressed in a fluid (normally oil) to give uniform compaction through the body. Shapes of much greater complexity can be made than in die pressing. Isostatic pressing is of two types; Cold isostatic pressing and hot isostatic pressing.

3.4.3 Extrusion

By mixing the ceramic powder with polymers or polymer solutions, the coefficient of friction between the powder particles can be reduced sufficiently that a compact can be uniformly sheared and does not behave like a dilatant solid. In clays this can be achieved by adding water. Such a compact can then be extruded through a die and can give very complex shapes.

3.4.4 Injection Molding

A powder/polymer mix described above can also be injection molded in a die in the same way as plastic and metal parts are made. Very complex shapes such as turbocharger rotors can be made in this way.

3.4.5 Slip casting

Here a ceramic powder is mixed with a few drops of dispersant (such as sodium lingo sulphonate) in some fluid (often water) to give a suspension of ceramic particles. Paint is a good example. The suspension is then poured into a porous mold. The fluid is then drawn out of the suspension and into the mold leaving a layer of powder compact against the wall. Any excess slip can be removed leaving a hollow component.

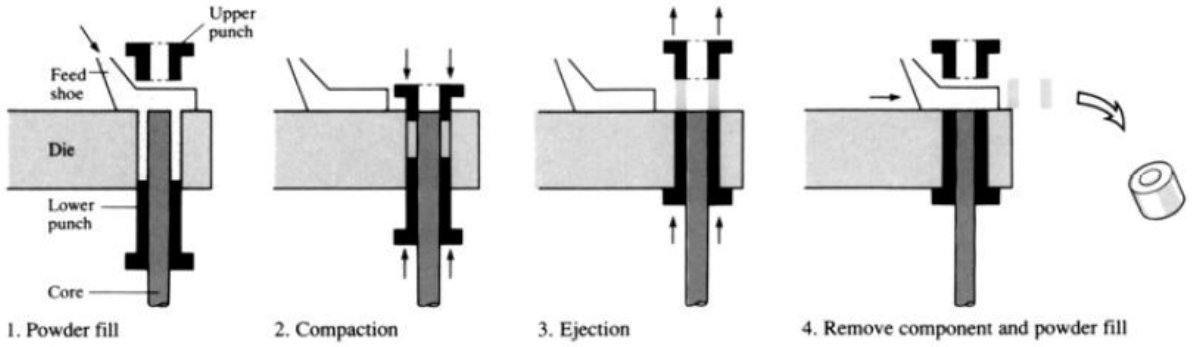

Figure 3.2 Schematic of *Uniaxial pressing*

3.5 Sintering

Sintering is the process by which a powder compact is transformed to a strong, dense ceramic body upon heating.

In an alternate definition given by Herring,

sintering is ". . . understood to mean any changes in shape which a small particle or a cluster of particles of uniform composition undergoes when held at high temperature."

Sintering is a complex phenomenon in which several processes are occurring simultaneously.

The main goal is how to consistently obtain theoretical density at the lowest possible temperature. The main difficulty in achieving this goal, however, lies in the fact that the driving force for sintering is quite small, usually on the order of a few joules per mole, compared to a few kilojoules per mole in the case of chemical reactions.

Sintering can occur in the presence or absence of a liquid phase. In the former case, it is called liquid-phase sintering, where the compositions and sintering temperatures are chosen such that some liquid is formed during processing. This process is of paramount importance and is technologically the process of choice. In the absence of a liquid phase, the process is referred to as solid-state sintering. This chapter is mainly devoted to understanding the science behind the sintering process.

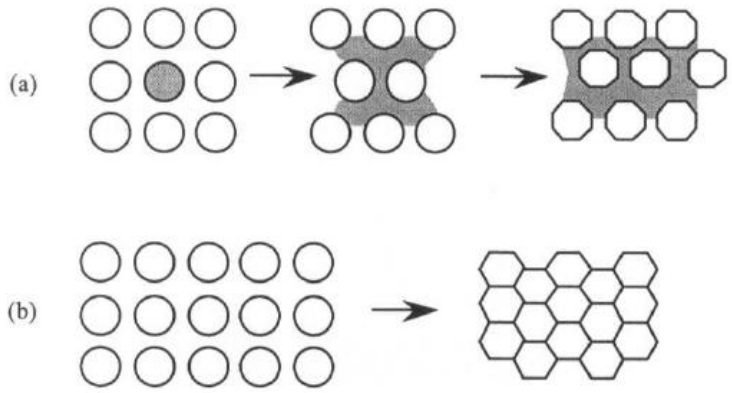

Figure 3.3(a) Liquid phase sintering (b) solid phase sintering

3.6 Solid-State Sintering

The macroscopic driving force operative during sintering is the reduction of the excess energy associated with surfaces. This can happen by (1) reduction of the total surface area by an increase in the average size of the particles, which leads to coarsening (Fig. 3.4b), and/or (2) the elimination of solid/vapor interfaces and the creation of grain boundary area, followed by grain growth, which leads to densification (Fig. 3.4a).

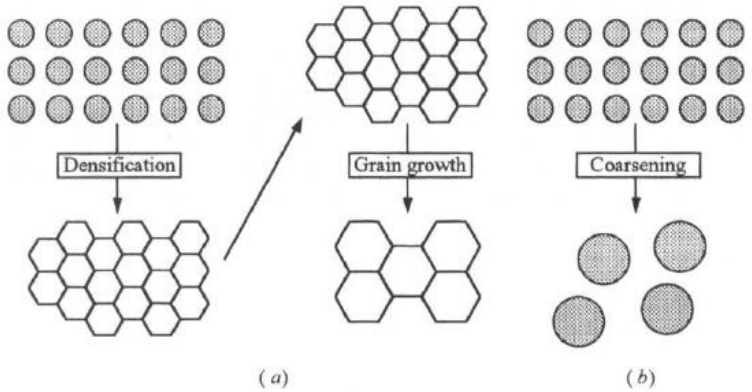

Figure 3.4Schematic of two possible paths by which a collection of particles can lowerits energy, *(a)* Densification followed by grain growth. In this case, shrinkage of thecompact has to occur, *(b)*Coarsening where the large grains grow at the expense of thesmaller ones.

These two mechanisms are usually in competition. If the atomic processes that lead to densification dominate, the pores get smaller and disappear with time and the compact shrinks. But if the atomic processes that lead to coarsening are faster, both the pores and grains get larger with time.

3.6.1 Atomic Mechanisms Occurring during Sintering

There are basically five atomic mechanisms by which mass can be transferred in a powder compact:

1. Evaporation—condensation, depicted as path 1 in Fig. 3.5a.

2. Surface diffusion, or path 2 in Fig. 3.5a.

3. Volume diffusion. Here there are two paths. The mass can be transferred from the surface to the neck area — path 3 in Fig. 3.5a — or from the grain boundary area to the neck area — path 5 in Fig. 3.5b.

4. Grain boundary diffusion from the grain boundary area to the neck area— path 4 in Fig. 3.5b.

5. Viscous or creep flow. This mechanism entails either the plastic deformation or viscous flow of particles from areas of high stress to low stress and can lead to densification.

Consider now which of these mechanisms leads to coarsening and which to densification.

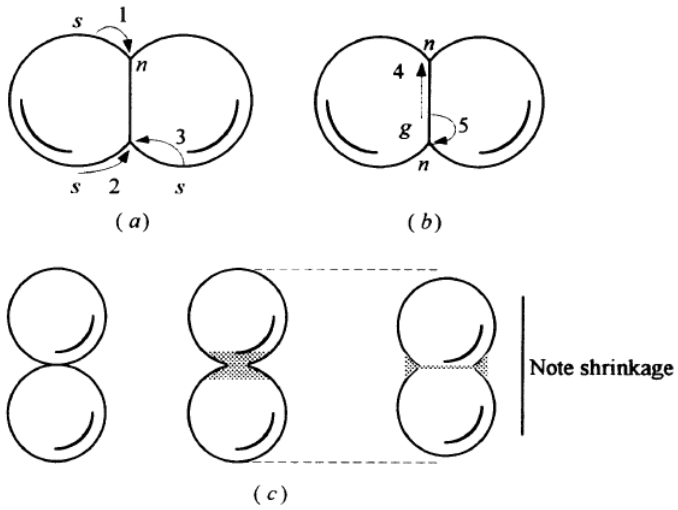

Figure 3.5Basic atomic mechanisms that can lead to *(a)* coarsening and change in pore shape and *(b)* densification. *(c)* Thought experiment illustrating how removal of material from the area between particles into the pore leads to shrinkage and densification.

3.6.1.1 Coarsening

At the outset, it is important to appreciate that any mechanism in which the source of material is the surface of the particles and the sink is the neck area cannot lead to densification, because such a mechanism does not allow the particle centers to move closer together. Consequently, evaporation-condensation, surface diffusion, and lattice diffusion from the surface to the neck area cannot lead to densification. They do, however, result in a change in the shape of the pores, a growth in the neck size, and a concomitant increase in compact strength. Moreover, the smaller grains, with their smaller radii of curvature, will tend to "evaporate" away and plate out on the larger particles, resulting in a coarsening of the microstructure. The driving force in all cases is the partial pressure differential associated with the local variations in curvature.

3.6.1.2Densification

If mass transfer from the surface to the neck area or from the surface of smaller to larger grains does not lead to densification, other mechanisms have to be invoked to explain the latter.

For densification to occur the source of material has to be the grain boundary or region between powder particles, and the sink has to be the neck or pore region.

Atomistically, both mechanisms involve the diffusion of ions from the grain boundary region toward the neck area, for which the driving force is the curvature-induced vacancy concentration.

Because there are more vacancies in the neck area than in the region between the grains, a vacancy flux develops away from the pore surface into the grain boundary area, where the vacancies are eventually annihilated. Needless to say, an equal atomic flux will diffuse in the opposite direction, filling the pores.

3.7 Sintering stages

Coble[2] described a sintering stage as an "interval of geometric change in which pore shape is totally defined (such as rounding of necks during the initial stage sintering) or an interval of time during which the pore remains constant in shape while decreasing in size." Based on that definition, three stages have been identified: an initial, an intermediate, and a final stage.

3.7.1 Initial stage

During the initial stage, the interparticle contact area increases by neck growth (Fig. 3.6b) from 0 to «0.2, and the relative density increases from about 60 to 65 percent.

3.7.2Intermediate stage

The intermediate stage is characterized by continuous pore channels that are coincident with three-grain edges (Fig. 3.6c). During this stage, the relative density increases from 65 to about 90 percent by having matter diffuse toward, and vacancies away from the long cylindrical channels.

3.7.3 Final stage

The final stage begins when the pore phase is eventually pinched off and is characterized by the absence of a continuous pore channel (Fig. 3.6d). Individual pores are either of lenticular shape, if they reside on the grain boundaries, or rounded, if they reside within a grain. An important characteristic of this stage is the increase in pore and grain boundary mobilities, which have to be controlled if the theoretical density is to be achieved.

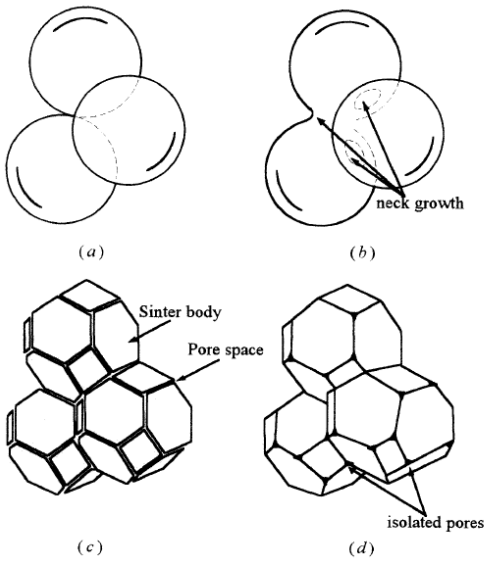

Figure 3.6(a) Initial stage of sintering model represented by spheres in tangential contact, *(b)* Near end of initial stage; spheres have begun to coalesce, *(c)* Intermediate stage; grains adopted shape of dodecahedra, enclosing pore channels at grain edges, (d) Final stage; pores are tetrahedral inclusions at corners where four dodecahedra meet.

3.8 Factors Affecting Solid State Sintering

Typically a solid-state sintered ceramic is an opaque material containing some residual porosity and grains that are much larger than the starting particle sizes.

3.8.1 Temperature

Since diffusion is responsible for sintering, clearly increasing temperature will greatly enhance the sintering kinetics, because D is thermally activated. The activation energies for bulk diffusion are usually higher than those for surface and grain boundary diffusion. Therefore, increasing the temperature usually enhances the bulk diffusion mechanisms which lead to densification.

3.8.2 Green density

Usually a correlation exists between the green (prior to sintering) density and the final density, since the higher the green density, less pore volume has to be eliminated.

3.8.3 Uniformity of green microstructure

More important than the green density is the uniformity of the green microstructure and the lack of agglomerates.

3.8.4 Atmosphere

The effect of atmosphere can be critical to the densification of a powder compact. In some cases, the atmosphere can enhance the diffusivity of a rate-controlling species, e.g., by influencing the defect structure. In other cases, the presence of a certain gas can promote coarsening by enhancing the vapor pressure and totally suppressing densification.

3.8.5 Impurities

The role of impurities cannot be overemphasized. The key to many successful commercial products has been the identification of the right pinch of magic dust. The role of impurities has been extensively studied, and to date their effect can be summarized as follows:

3.8.5.1 Sintering aids.

They are purposefully added to form a liquid phase. It is also important to note that the role of impurities is not always appreciated. The presence of impurities can form low-temperature eutectics and result in enhanced sintering kinetics, even in very small concentrations.

3.8.5.2. Suppress coarsening

Suppress coarsening by reducing the evaporation rate and lowering surface diffusion.

3.8.5.3. Suppress grain growth

Suppress grain growth and lower grain boundary mobility.

3.8.5.4. Enhance diffusion rate.

Once the rate-limiting ion during sintering is identified, the addition of the proper dopant that will go into solution and create vacancies on that sublattice should, in principle, enhance the densification kinetics.

3.8.6 Size distribution

Narrow grain size distributions will decrease the tendency for abnormal grain growth.

3.8.7 Particle size

Since the driving force for densification is the reduction in surface area, the larger the initial surface area, the greater the driving force. Thus it would seem that one should use the finest initial particle size possible, and while in principle this is good advice, in practice very fine particles pose serious problems. As the surface/volume ratio of the particles increases, electrostatic and other surface forces become dominant, which leads to agglomeration. Upon heating, the agglomerates have a tendency to sinter together into larger particles, which not only

dissipates the driving force for densification but also creates large pores between the partially sintered agglomerates which are subsequently difficult to eliminate.

References:

1. W. H. Rhodes, J. Amer. Cer. Soc., 64:19 (1981).
2. R. L. Coble. J. Appl. Phys.. 32:787-792 (1961); R. L. Coble. J. Appl. Phys..36:2327 (1965).
3. Wang, P.E. and Chaki T.K., 1993, Sintering behavior and mechanical properties of hydroxyapatite and di-calcium phosphate, J. Material Science: Mat. Med., pages 150-158
4. Van Landyut, P. Li. F., Keustermans J.P., Sterydio J.M., 1995, The influence of high sintering on the mechanical properties of hydroxyapatite, J. Material Science: Mat. Med., pages 6,8-13
5. Irita I.H., Castano V.M., Wilkinson D.S, 1995, Synthesis and processing of hydroxyapatite tapes with controlled porosity, J. Material Science: Mat. Med., pages 19-23
6. Zhou J., Zhang X., Chen J., Zeng S., D. Groot K., 1993, High temperature of characteristics of hydroxyapatite, J. Material Science: Mat. Med., pages 83-85
7. R. Kumar, K.H. Prakash, P. Cheang, K.A. Khor,2005 Acta Materialia‘53 2327–2332.
8. S. Ramesh, C.Y. Tan, I. Sopyan, M. Hamdi,W.D. Teng,W.D. Teng, (2007) Advanced Materials8 124–130.
9. M. Mazaheri, A.M. Zahedi, S.K. Sadrnezhaad, (2008) Journal of the American CeramicSociety 91 56–63.
10. Y.W. Gu, N.H. Loh, K.A. Khor, S.B. Tor, P. Cheang, (2002) Biomaterials 23 37–43.
11. X. Guo, P. Xiao, J. Liu, Z. Shen, (2005) Journal of the American Ceramic Society 88 1026–1029.
12. A.Weibel, R. Bouchet, R. Denoyel, P. Knauth, (2007) Journal of European Ceramic Society 27 2641–2646.
13. S Sarfrazet al, Adv Materials Res; Vol 264-265, 2011, PP 1370-1375

Chapter 4:

Experimental Methods for Compaction and sintering

Chapter 4: Experimental Methods for Compaction and sintering

4.1 Aim and Scheme for work

The aim of this work includes:

1. Investigate the effect of different compaction loads on the green density and sintered density of Nano crystalline HA.
2. To study the effect of different sintering temperatures on the densification and mechanical properties of HA
3. Observe the effect of different sintering times during sintering on the sintered density of HA
4. Observe the variation of hardness and flexural strength by increasing sintering temperature

4.2 Compaction of HA Powder

The as received powder was initially grinded in mortar & pestle to get a uniform size. The mortar & pestle used for grinding HA was Agate Mortar & Pestle. The reason for using Agate Mortar &pestle was that it had greater hardness than HA so no chances of getting scratched during grinding and mixing of any impurities from mortar & pestle.

The ground HA powder was compacted under a uniaxial hydraulic press (12 tons) under three different compaction loads; 1 ton, 2 ton and 5 ton. At higher compaction loads the pellet was likely to crack during sintering and was thus avoided.

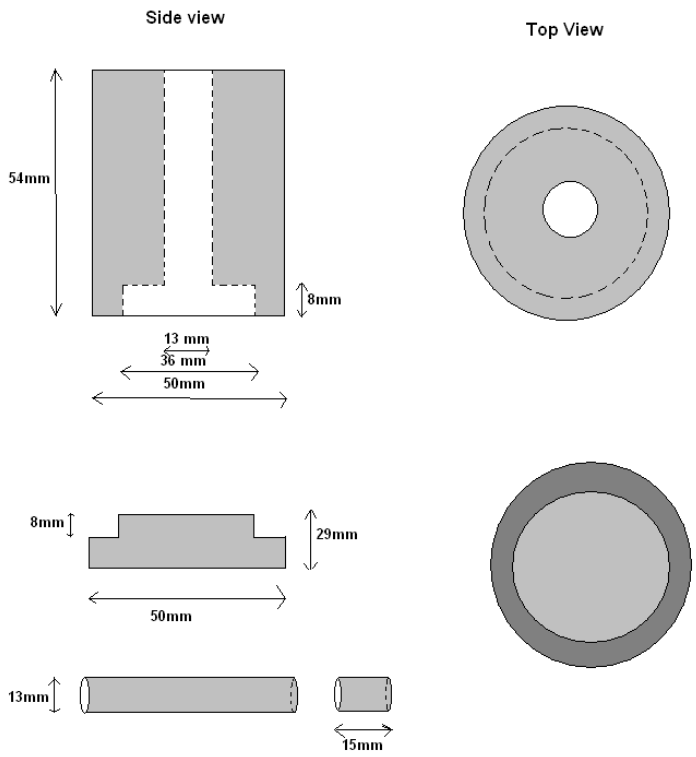

Figure 4.2 Design of the compaction die

The compaction time during the application of these compaction loads was selected for 2 to 3 minutes. Compaction time more than 3 minutes had no effect on the resultant green density of the pellets. So the optimum time for compaction under a hydraulic press was selected as 3 minutes.

The powder was compacted in a die with a diameter of 13 mm. The powder initially taken for making each pellet was 1 gram. The thickness of the pellets varied with the compaction loads. The average thickness of the pellet was 4 to 5 mm whereas the diameter of the pellets remained constant.

The internal surface of the die was lubricated by Stearic acid. Stearic acid was mixed in ethanol. The flow ability of HA powder during compaction was good as it compacted without any binder. Proper care should be taken during compaction as the lubricating oil of the press might leak and get on the die.

Proper care was taken during the handling of the green pellet as it gets easily break and edges are chipped off.

4.3 Sintering

Sintering of the green pellets was done in a muffle furnace KSL 1600X with different sintering temperatures and time.

Heating rate was selected as 2°C/minute on initial sintering up to a temperature of 700°C and then a fast heating rate of 5°C/minute was selected. This was done to avoid the crack formation during sintering of the green pellets. Also this change of heating rate shortened the overall sintering time for each sintering cycle.

The sintering temperature was selected in a range of 850°C to 1250°C to study the sintering behavior of HA. Three temperatures were selected; 850°C, 1050°C and 1250°C. The temperature of 850°C was selected as normally the HA sintering starts from this temperature and maximum sintered density is achieved at 1250°C.

Some results show that HA is found stable in moist or dry air up to 1200°C and does not decompose,[1-4] other authors report that stoichiometric HA, after a DE hydroxylation process (which occurs gradually but in two steps, i.e. at about 900°C and at 1300±1400°C), starts to decompose into secondary phases at temperature in the range 1350±1500°C. [5-6]

Soaking time at these sintering temperatures was varied from 1 to 3 hours.

4.4 Characterization Techniques Used

A plethora of techniques have been developed to characterize biomaterials, some of these are quantitative analysis and some are qualitative. Quantitative procedures produce a numerical measure of a property (in absolute or relative units), whereas qualitative experiments give a general overview of the property of interest without supplying a numerical value. Quantitative characterization of degradative and bulk properties often involves a form of spectroscopy,

chromatography or mechanical testing. Spectroscopy measures how compounds absorb different type of energies while chromatography uses various means to physically separate molecules on the basis of chemical characteristics such as charge or size. Mechanical assessment of materials is performed with a mechanical testing frame that allows for controlled loading of the sample by pulling, pushing or bending it at a preset rate [7]. Observing surface under microscope is a qualitative technique. Many of the surfaces are chemically active so they need special preparation procedures or equipment to prevent contamination. However despite these limitations a wide range of surface characterization methods has been developed. Many methods involve modification of techniques for bulk properties. Qualitative methods like various types of microscopy can provide valuable information on the structure and topography of the biomaterial surface. Following techniques were employed for characterization of samples prepared by set of experiments;

(1) X-Ray Diffraction

(2) Scanning Electron Microscopy

(3) FTIR Spectroscopy

(4) Thermo gravimetric Analysis

(5) Vickers Hardness Testing

(6) Archimedes Method for density measurement

4.4.1 X-Ray Diffraction

Rather than measuring how the absorbance of X-rays affects the sample as in spectroscopic techniques this method examines how X-rays are diffracted from atoms in a material. X-ray diffraction was used here to determine structures of crystals and its indexing to check phase purity level and phase transitions. Because the wave length of X-rays (0.5-50Å) is similar to the distance between atoms in solid so these rays are ideal to explore structural details of crystals. Diffraction of X-rays occurs when incident rays are scattered by atoms in a way that reinforces the waves according to Bragg's law.

$$2dSin\theta = n\lambda$$

XRD analysis was carried out using STOE diffractometer at SCME NUST, using Cu Kα monochromatic radiation at scan range of 20° to 80° with step size of 0.4 and stay time at each step of 4sec. Silicon was used to calibrate the instrument. XRD plots obtained were analyzed at the software of same machine to get information about phases present, crystallinity and crystallite sizes.

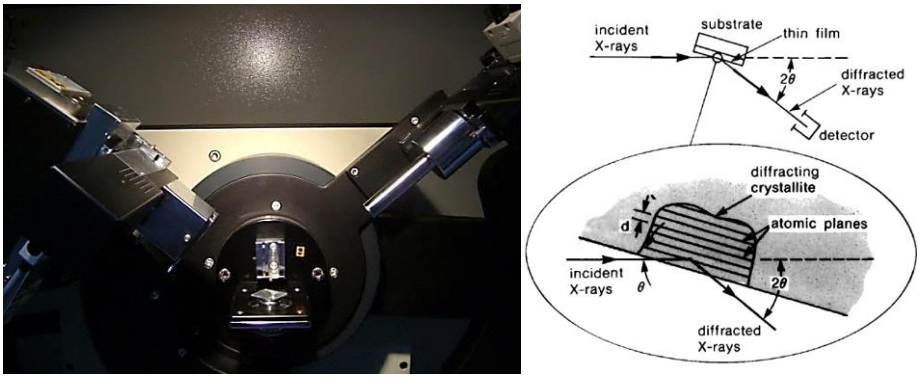

Figure 4.3: (a) XRD machine at SCME; (b) Basic features of a typical XRD experiment

4.4.2 Scanning Electron Microscopy

SEM analysis was performed using JEOL Japan, JSM 6490A analytical scanning electron microscope, the resolution of this SEM can approach a few nm and it can operate at magnifications that are easily adjusted from about 10-300,000. Along with topographical information it can also provide composition of the surface being observed by energy dispersive spectroscopy (EDX) using the fluorescence X-rays produced in the material due to interaction of highly accelerated electrons with the material. As the samples observed were of ceramics so were not able to conduct charge of striking electron beam and would have started deflecting further incoming electrons due to charge accumulation and resulting image turn blurred. To combat this problem all of the powder and sintered pellet samples were initially coated with 200 Å thick layer of gold to make them conductive with the help of JFC 1500 ion sputtering device. SEM analysis was conducted to get information about particles size, shape surface morphology, packing and composition.

Figure 4-4(a) shows the JSM 6490LA SEM present in School of Chemical and Materials Engineering, National University of Science and Technology, Islamabad. Figure 4-4(b) shows schematic of a typical SEM.

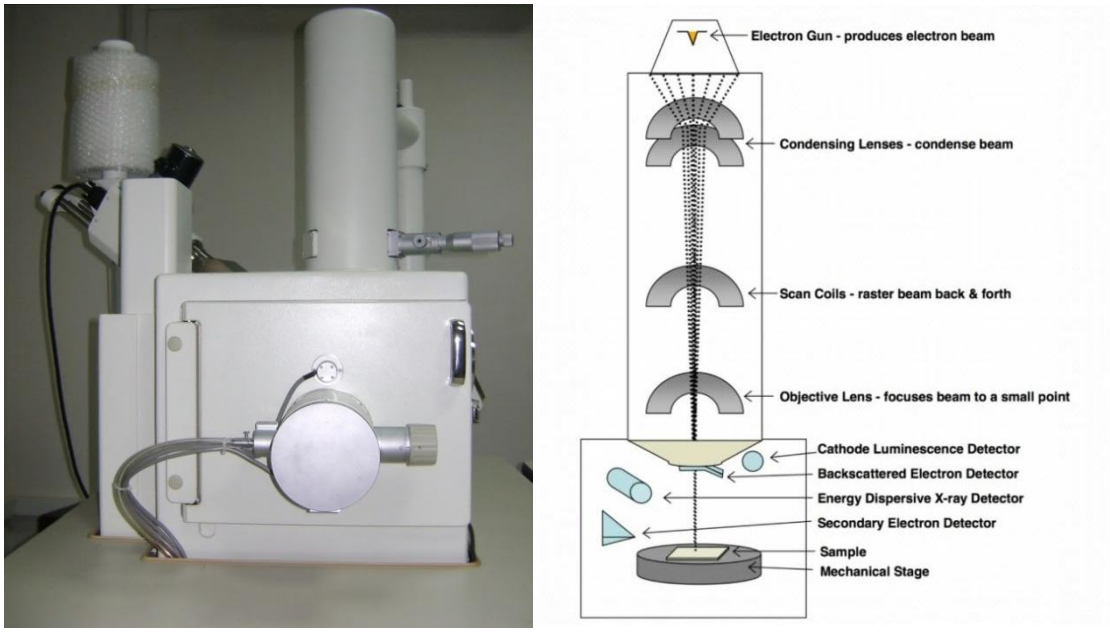

Figure: 4.4 (a) JSM 6490LA present at SCME; (b) SEM Schematic.[3]

4.4.3 FTIR Spectroscopy

IR spectroscopy measures the interaction of infra-red radiations with the molecules of the material. For a material to be susceptible to IR radiations it must possess a permanent dipole and those lacking this property are transparent to IR spectroscopy. A polar bond can be thought of as oscillating or vibrating with a certain frequency. Since this is occurring in three dimensions there are numbers of vibrations possible for any given bond including stretching, bending and rocking movements. If the frequency of IR radiation matches with this frequency of vibration then there is reinforcing action and amplitude of vibration or oscillation increases but the frequency of vibration remains same. As there are many type of bonds present in any material so there will be interaction at many frequencies giving a finger print of that material specific to that only. Thus IR spectroscopy gives information about the functional groups present and nature of bonds.

FTIR spectra were collected over the range of 400-4000 cm^{-1} (Perkin Elmer, USA). Test samples prepared for this characterization were in pallet form. These pallets were made by mixing

analytical grade Potassium Bromide (KBr) and synthesized powder in ratio 99:01 then pressing in hydraulic press at a pressure of 5 ton. FTIR spectra were used to check the purity of material.

4.4.4 Thermo Gravimetric Analysis (TGA)

In thermo gravimetric analysis weight of the specimen is calculated as a function of the temperature of that material. The sample is heated at a predefined heating rate in reactive, oxidizing or inert atmosphere. The sample weight or percent weight is plotted against the temperature profile. Whenever material will react with environment or degrades the weight changes occur. TGA measurements of the samples were carried out at heating rate of 10°C /min in nitrogen atmosphere (Perkin Elmer, USA) between 50°C and 1400°C.

TGA analysis was carried out to find the thermal losses, de hydroxylation and decomposition of Hydroxyapatite.

4.4.5 Vickers Hardness Testing

The Vickers hardness test uses a square base diamond pyramid as an indenter, the included angle between the opposite face of pyramid is 136°. Vickers hardness number is calculated by dividing load with the surface area of the indentation, this area is calculated by the length of the diagonals of the impression. Vickers hardness number (VHN) also called as diamond pyramid hardness (DPH) can be calculated by the following equation;

$$DPH = \frac{\left\{\frac{2Psin\theta}{2}\right\}}{L^2} = \frac{1.854P}{L^2}$$

Where

P= applied load, kg

L= average length of diagonal, mm

θ = angle between opposite faces of diamond = 136°

Vickers hardness is usually preferred over other hardness tests as this provides a continuous scale from very soft to hard materials [8].

Vickers harness testing was performed on micro hardness tester at a load of 1.0 kg and dwell time of 15 seconds and three reading were taken for each sample. This test was performed to calculate and compare the hardness sintered pallets of pure HA at different compaction loads and sintering temperatures.

4.4.6Archimedes method for density measurement

According to Archimedes Principle when an object is immersed in a fluid, the fluid exerts on the object a force whose magnitude is equal to the weight of the displaced fluid and whose direction is opposite the force of gravity.

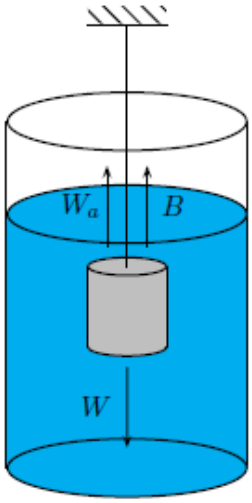

Figure 4.5: Archimedes Principle

Consider the specific case of an object suspended from a string while being immersed in a container of water, as depicted in Figure below. Because the object is in static equilibrium, the net force on the object is zero so that

$Wa + B - W = 0$ (1)

Where Wa is the tension in the string (the apparent weight of the object),

& W is the weight of the object.

The buoyant force B is

$$B = \rho_{water} V g \qquad (2)$$

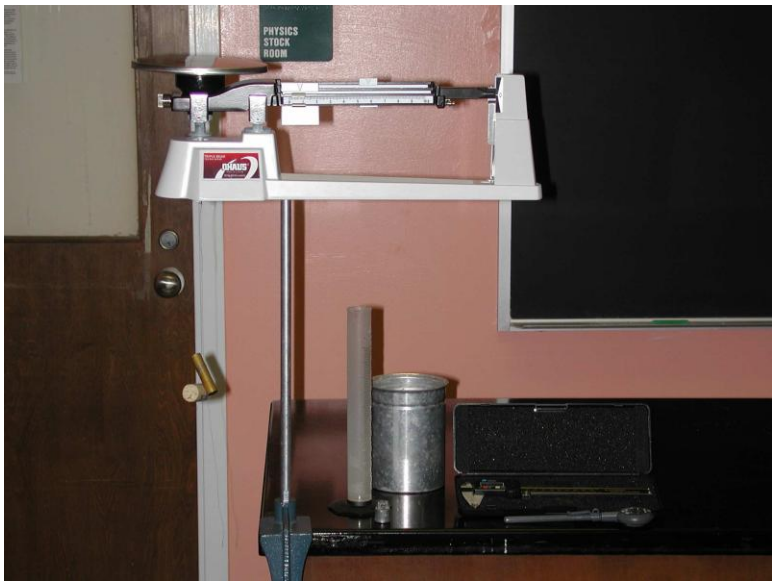

Figure: 4.6: Apparatus used for measuring Density by Archimede's Method

In Equation 2 V is the volume of the object, ρ_{water} is the density of water, and g is the acceleration of gravity. It can be shown using Equations 1 and 2 that the density of the object ρ satisfies the relationship

$$\rho = \frac{M\rho_{water}}{M - M_a} \qquad (3)$$

The values obtained are then compared to those obtained by the less precise method of calculating the density directly using the relationship

$$\rho = \frac{M}{V} \qquad (4)$$

References:

1. Wang, P. E. and Chaki, T. K., Sintering behavior and mechanical properties of hydroxyapatite and dicalcium phosphate. J. Mat. Sci.: Mat. Med., 1993, 4, 150±158.
2. Van Landuyt, P., Li, F., Keustermans, J. P., Streydio, J. M. and Delannay, F., The influuence of high sintering temperature on the mechanical properties of hydroxyapatite. J. Mat. Sci.: Mat. Med., 1995, 6, 8±13.
3. Arita, I. H., Castano, V. M. and Wilkinson, D. S., Synthesis and processing of hydroxyapatite ceramic tapes with controlled porosity. J. Mat. Sci.: Mat. Med., 1995, 6, 19±23.
4. Zhou, J., Zhang, X., Chen, J., Zeng, S. and De Groot, K., High temperature characteristic of synthetic hydroxyapatite. J. Mat.Sci.: Mat. Med., 1993, 4, 83±85.
5. Zyman, Z., Cao, Y. and Zhang, X., Periodic crystallization effectin the surface layers of coatings during plasma spraying ofhydroxyapatite. Biomaterials, 1993, 14, 1140±1144.
6. Wang, C. K., Ju, C. P. and Chern Lin, J. H., Effect of dopedbioactive glass on structure and properties of sintered hydroxyapatite. Mat. Chem. Phys, 1998, 53, 138±149.
7. R. Kumar, K.H. Prakash, P. Cheang, K.A. Khor,2005 Acta Materialia‘53 2327–2332.
8. S. Ramesh, C.Y. Tan, I. Sopyan, M. Hamdi,W.D. Teng,W.D. Teng, (2007) Advanced Materials8 124–130.
9. M. Mazaheri, A.M. Zahedi, S.K. Sadrnezhaad, (2008) Journal of the American CeramicSociety 91 56–63.
10. Y.W. Gu, N.H. Loh, K.A. Khor, S.B. Tor, P. Cheang, (2002) Biomaterials 23 37–43.
11. X. Guo, P. Xiao, J. Liu, Z. Shen, (2005) Journal of the American Ceramic Society 88 1026–1029.
12. A.Weibel, R. Bouchet, R. Denoyel, P. Knauth, (2007) Journal of European Ceramic Society 27 2641–2646.

Chapter 5
RESULTS AND DISCUSSIONS

CHAPTER 5 Results & Discussions

The results obtained from different set of experiments conducted during this research project are discussed in this chapter.

5.1 Initial Characterization:

The first step during the project was to study the morphology, particle size, crystallite size, chemical groups attached, decomposition behavior, phase stability and phase purity of the as received HA powder. For this reason, X-Ray diffraction (XRD), Scanning electron Microscopy (SEM), Thermo gravimetric Analyzer (TGA/DTA) and FTIR Spectroscopy were done on as received powder prior to sintering.

5.1.1 XRD Analysis:

The XRD Pattern of as received HA powder is shown in the figure below. All Diffraction peaks could be perfectly indexed to hexagonal HA with lattice constants a= 9.42Å and c= 6.879Å (JCPDS card No. 00-074-0565). The results apparently indicate that the powder consists of hydroxyapatite phase with no or insignificant amount of impurities. The crystallite size of the as received HA is calculated by the Scherer's Formula [1] as follows

$$t = \frac{0.9\lambda}{\beta\cos\theta}$$

Where t is the crystallite size of the as received HA, λ is the wavelength of Cu Kα radiation (1.54Å), β is the intensity of peaks at full width half maximum (FWHM) and θ is the Bragg's angle.

The average crystallite size as calculated by this formula was 15nm. No other phases such as α-TCP and β-TCP were observed confirming the phase purity of HA.

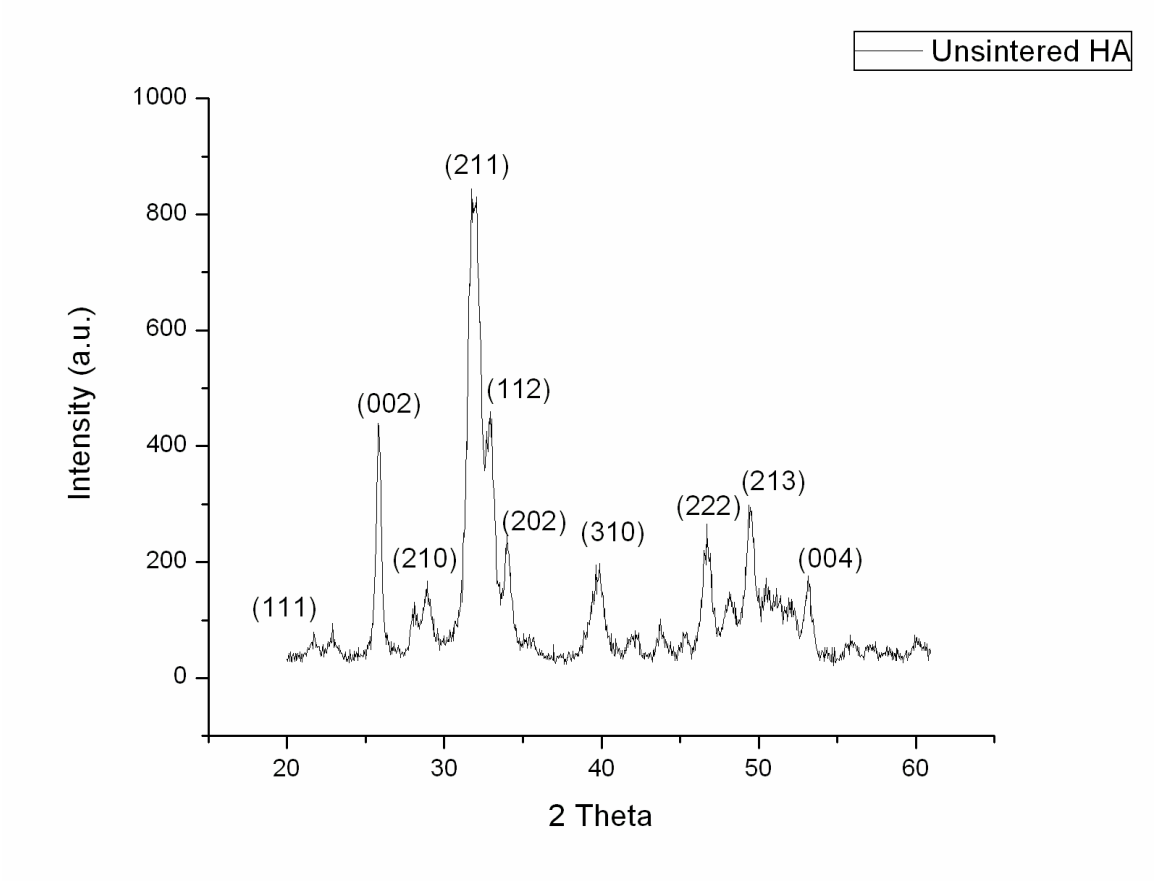

Figure 5.1 XRD Pattern of un-sintered HA

5.1.2 FTIR spectroscopy:

The FTIR spectrum of as received HA is shown below in Figure below. This spectrum reveals the characteristic bands of HA along with some additional bands that are ascribed to impurity ions (CO_3^{-2}, HPO_4^{2-}) and some associated water. Band at 1417 cm^{-1} is indicates v3 vibration of CO_3^{-2}ions. The band at 873 cm^{-1} is attributed to arise due to the presence of HPO_4^{2-}. The band at 963 cm^{-1} is due to the v1 symmetric stretching of PO_4^{3-} ions. The band at 873 cm^{-1} is due to the v2 vibration of CO_3^{-2} ions. The bands at 602 and 564 cm^{-1} are attributed to v4 bending mode of PO_4^{3}. The broad band from 3300-3700 cm^{-1} is due to stretching mode of hydrogen bonded water molecules and that at 1639 cm^{-1} derives from bending mode of water molecules. The sharpness of band at 564 cm^{-1} indicates a well crystallized HA.

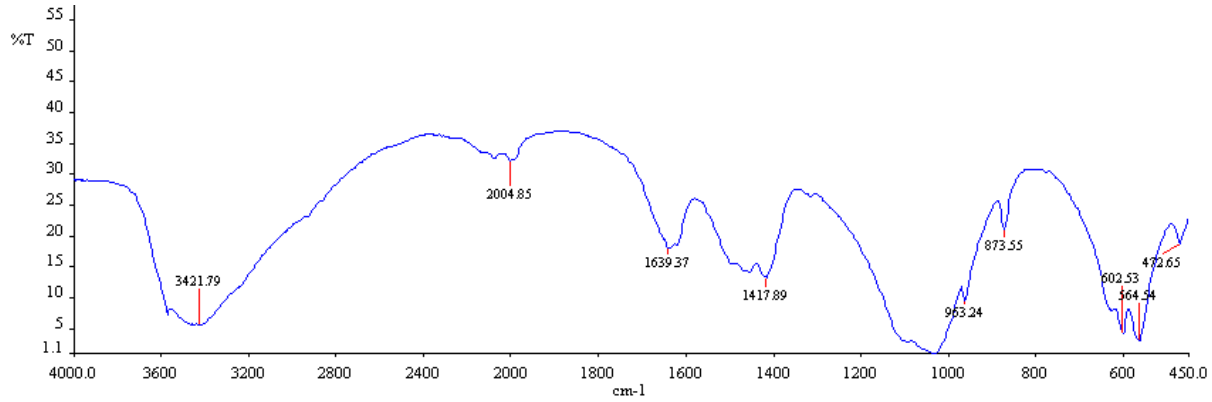

Figure 5.2 FTIR Spectrum of Un-sintered HA powder

5.1.3 SEM Analysis:

The sample for SEM was prepared by dispersing 0.2 g of HA powder in 100 ml of de-ionized water by sonication for 30 minutes. Then a drop of solution was placed over stub followed by drying of water leaving HA particle sticking to stub. A few particles are visible in image as solution was made very dilute in order to properly disperse the nanoparticles. Particles morphology appears to be spherical with size ranging from 30 to 60 nm.

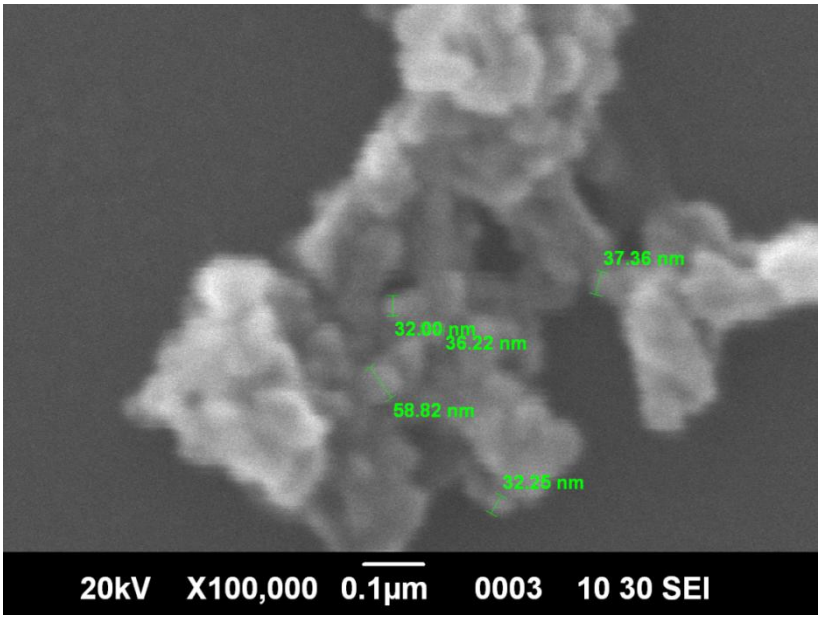

Figure 5.3 SEM micrograph of un-sintered Hydroxyapatite

5.1.4 Thermo gravimetric Analysis:

TGA graph shows high thermo gravimetric stability with no weight loss of as received HA. The weight gain visible in the plot is due to systematic error of the equipment which needs to be recalibrated. DTA plot gives valuable information about phase changes if any with the increase of temperature. Initial endothermic region up to 200°C is due to loss of moisture and organics that may be present. Then thermal arrest is observed up to 400°C. Now beyond 400°C de-hydroxylation starts which is highest at 800°C. This de-hydroxylation completes at about 1200°C. This made basis for selection of our sintering temperatures.

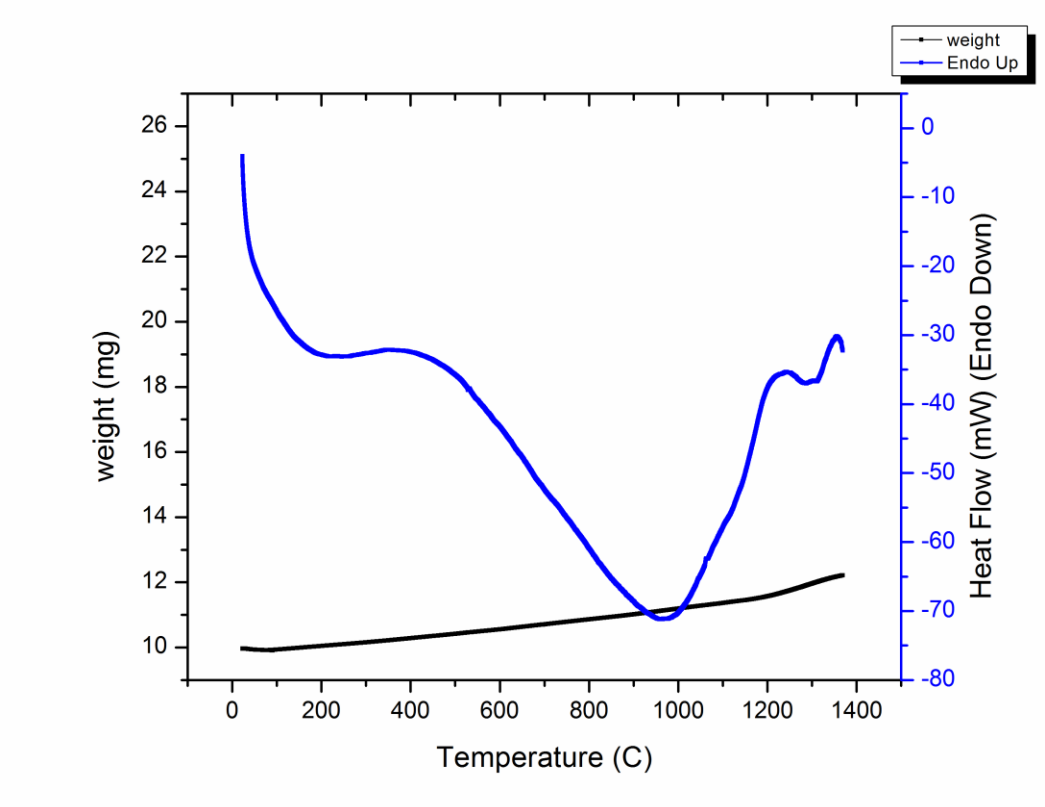

Figure 5.4 TGA/DTA of unsintered Hydroxyapatite

5.2 Effect of different compaction loads on the green density of HA powder

The effect of different compaction loads ranging from 1 ton to 5 ton was studied by uniaxially pressing the powder in a die having a diameter of 13 mm. 1 gram HA powder was weighed to be

used for making a single pellet. The powder was first grinded in Agate mortar & pestle to break the agglomerates and to uniform the powder size. The internal portion of the die was lubricated by Stearic acid dissolved in ethanol. The powder was compacted for 5 minutes in the die under the specific compaction load. It was observed that as the compaction load was increased the resultant green density was also increased. The green density was calculated by geometrical method by using Vernier Caliper and analytical weight balance. On average 5 readings for diameter and thickness were taken for each sample and their average value was taken. For each compaction load 5 samples were made and very little difference was observed. The theoretical density value of HA is 3.16 g/cm^3 and by using this value percent densification of the samples were calculated. The calculated values are tabulated below;

Table; 5.1 Effect of different compaction loads on green density

Compaction load (ton)	Mass used for making pellet (g)	Diameter of the compacted pellet (mm)	Thickness of the compacted pellet (mm)	Green Density (g/cm^3)	Theoretical density (g/cm^3)	% Green Densification
1	1	13	6.5	1.15	3.16	36%
2	1	13	5.7	1.28	3.16	40%
5	1	13	4.81	1.52	3.16	48%

It was observed that the green density increased with the increase in compaction load. The percent densification value for 1 ton compaction load was 36% and it increased by 4 % when compaction load was doubled. It further increased to 48% when compaction load was increased to 5 ton. It clearly shows that compaction load plays an important role in the green densification of the HA pellets. There is a difference of 12 % between the 1 ton and 5 ton compaction load values.

One more observation was made during compaction regarding the color of HA pellets. When the load was increased to 5 ton the color changed slightly from white to light green.

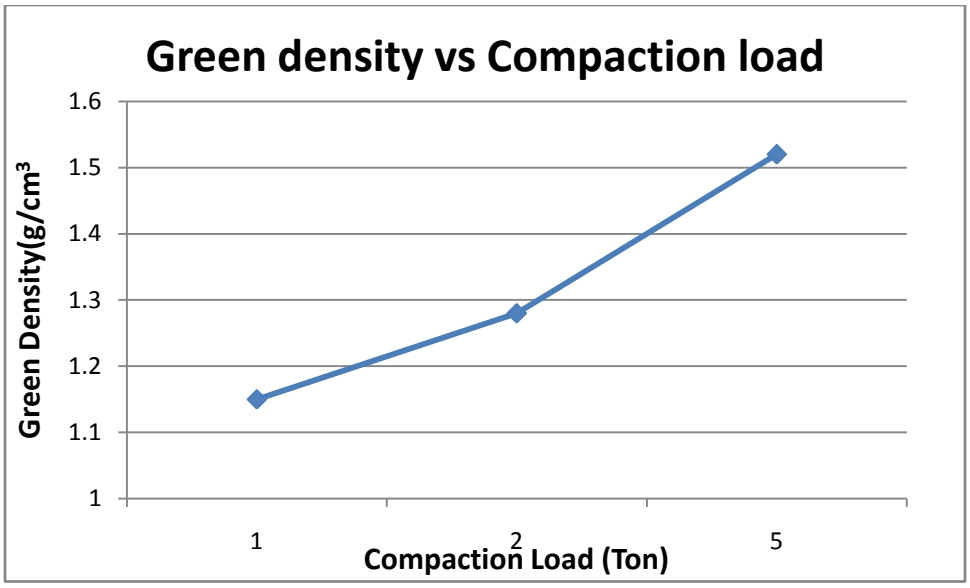

Figure 5.5 Effect of different compaction loads on green density

5.3 Parameters affecting Sintered Density:

Various parameters were studied to investigate the resultant effect on the sintered density. The following three parameters were studied:

- Effect of compaction load on sintered density
- Effect of Sintering temperature on Sintered Density
- Effect of Sintering time on Sintered Density

5.3.1 Effect of compaction load on sintered density

The compaction loads were varied from 1 ton to 5 ton and their effect on the resultant sintered densities were studied. These results were studied for three different temperatures 850˚C, 1050˚C and 1250˚C. The results are tabulated below:

Table 5.2 Effect of compaction load on sintered density

Compaction Load (ton)	Green density (g/cm3)	% Green densification	Sintered Density (g/cm3) (850˚C)	%Sintered Densification	Sintered density (g/cm3) (1050˚C)	% Sintered Densification	Sintered density (g/cm3) (1250˚C)	% Sintered Densification
1 ton	1.12	35%	2.70	85%	2.95	93%	3.12	98.7%
2 ton	1.28	40%	2.72	86%	2.91	92%	3.00	95%
5 ton	1.52	48%	2.85	90%	3.01	95%	3.10	98.1%

To describe the results for the effect of different compaction loads we will discuss in detail for each sintering temperature separately.

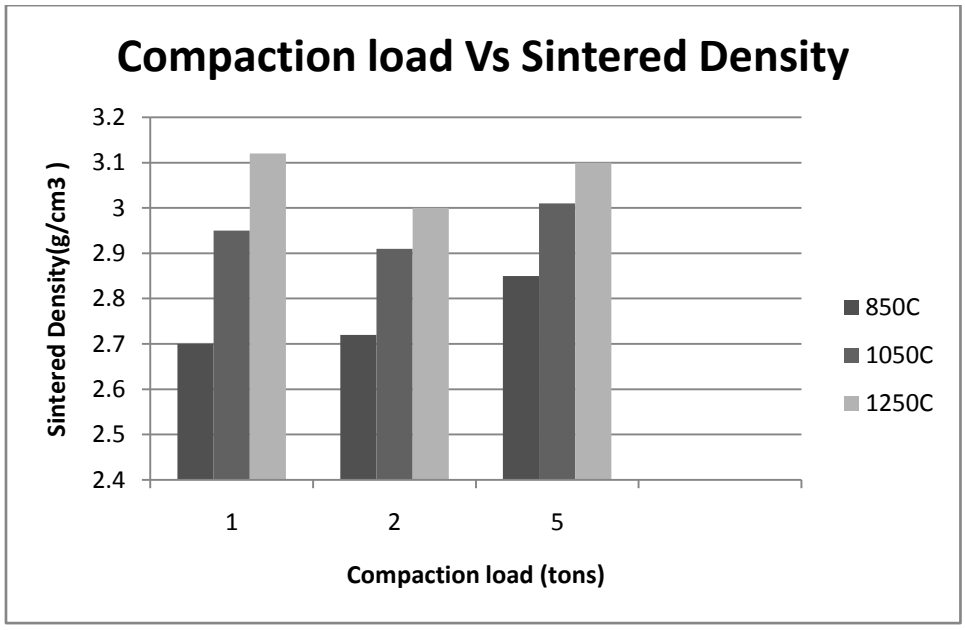

Figure 5.6 Effect of compaction load on sintered density

At 850˚C it was observed that the sintered density increased with the increase in compaction load. The sintered density increased from 85% at 1 ton load to 90% at 5 ton compaction load. There is a minor change in the sintered values of 1 ton and 2 ton compaction load.

At 1050˚C it was observed again that the sintered values were highest for the 5 ton compaction load and the overall sintered values increased from the previous values sintered at 850˚C. The sintered value difference between the three compaction loads also decreased. The percent sintered densification for 5 ton compaction load was only 2 % more than the 1 ton compaction load whereas previously at 850˚C it was 5 %. This shows that effect of load at higher sintering temperature plays very little role in densification of HA.

At 1250˚C no difference was observed in the sintered values between the two compaction loads at the extreme. The sintered values at higher temperatures are almost independent of compaction load.

5.3.2 Effect of Sintering temperature on Sintered Density

The sintering temperature was varied from 850˚C to 1050 ˚C and 1250 ˚C at different compaction loads to study the effect on the resultant sintered densities of hydroxyapatite. It was observed that the sintered density increased with the increase in the sintering temperature. The maximumsintered density was achieved for 1250 ˚C which is 98.7% of the theoretical density. The lowest sintered density was observed of the pellet which was sintered at 850 ˚C and it wasfound to be 85% of the theoretical density of hydroxyapatite.

Table 5.3 Effect of Sintering temperature on Sintered Density

Sintering Temp(˚C)	Sintered Density(g/cm3)	Sintered Density(g/cm3)	Sintered Density (g/cm3)
	1 ton load	2 ton load	5 ton load
850	2.70	2.72	2.85
1050	2.95	2.90	3.01
1250	3.12	3.0	3.10

The following plot shows that there is a linear trend in the increase of sintered density with the increase of sintering temperature of the HA pellets. The sintered density of the pellets compacted

at 5 ton and 2 ton was greater than pellets compacted at 1 ton except for the highest sintering temperature.

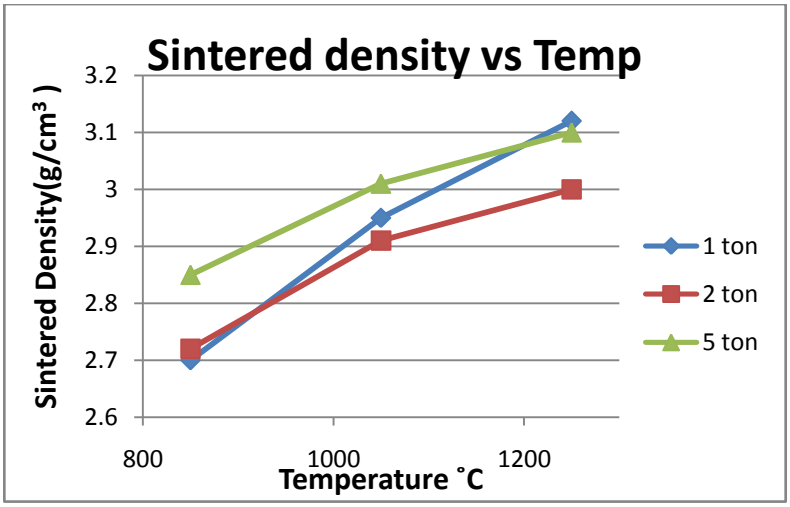

Figure 5.7 Effect of Sintering temperatures on Sintered Density

5.3.3 Effect of Sintering time on Sintered Density

The sintering time at these sintering temperatures was varied from 1 hour to 3 hours to investigate the effect of sintering time on the sintered density.

It was observed that with the decrease in sintering time at 850 ˚C from 3 hours to 1 hour, the resultant sintered density decreased tremendously from 85% to 50% of the theoretical density of HA. This occurred due to the incomplete sintering of HA at this temperature. It shows that the sintering just started at this temperature which would complete only by increasing the sintering time to 3 hours or sintering HA higher temperatures.

At 1050 ˚C, the sintered density decreased to 83% (at 1 hour sintering time) from 93% sintered densification which was achieved by sintering for 3 hours. This investigation showed us that at 1050 ˚C the sintering was 83% complete and it further can be increased by giving the proper time to get sintered densification more than 90%.

The effect of varying sintering time at 1250 ˚C from 3 hours to 1 hour showed a little decrease in sintered densification of only 6% and 4% sintered densification difference by varying sintering time from 3 hours to 2 hours. It showed that the sintering is in the final stage at 1250 ˚C and very little effect is observed in the final densification of HA.

Table 5.4 Effect of Sintering time on Sintered Density

Temp ˚C	Sintered Density at 1 hr	Sintered Density at 2 hrs	Sintered Density at 3 Hrs
850	1.58	-	2.8
1050	2.64	-	2.95
1250	2.92	2.98	3.12

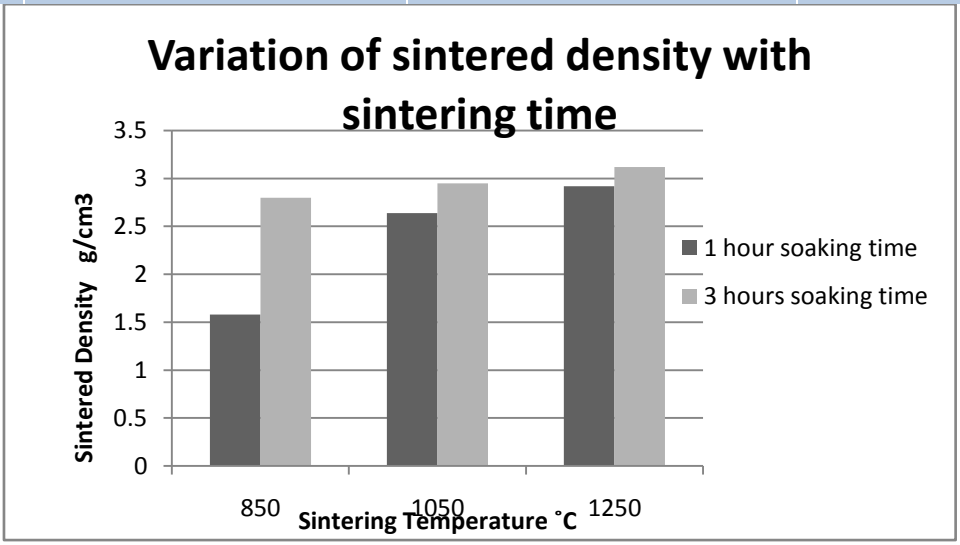

Figure 5.8 Effect of Sintering time on Sintered Density

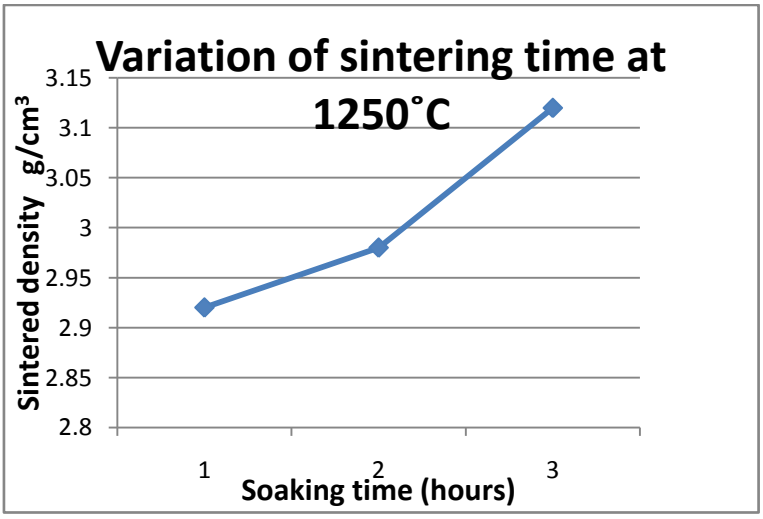

Figure 5.9 Variation of sintering time at 1250˚C

5.4 Parameters affecting Hardness:

Vickers harness testing was performed on micro hardness tester at a load of 1.0 kg and dwell time of 15 seconds and three readings were taken for each sample. This test was performed to calculate and compare the hardness of sintered pellets of pure HA at different compaction loads and sintering temperatures.

The resultant effect on the Vickers Hardness values of the following three main parameters was studied:

- Effect of compaction load on Vickers Hardness value
- Effect of sintered density on Vickers Hardness value
- Effect of Sintering temperature on Vickers hardness value
- Effect of Sintering time on Vickers hardness value

5.4.1 Effect of compaction load on Vickers Hardness value

The first parameter which was studied to observe the Vickers Hardness of Hydroxyapatite was the variation of compaction load. Three different compaction loads of 1 ton, 2 ton and 5 ton were applied on the HA pellets prior to sintering. Then the sintering was done at three different sintering temperatures of 850 ˚C, 1050 ˚C and 1250 ˚C. The sintering time was selected for 3 hours.

It was observed that as the compaction load is increased the hardness values are also increased. The results clearly show that at 850 ˚C the hardness value for 5 ton compaction load is much higher than 1 ton and 2 ton loads. The reason for increase in hardness value at higher compaction load is due to the initial higher values of green density which affects the sintering rate, thus increasing hardness values.

At 1050 ˚C there is no difference in the hardness values between 1 ton and 2 ton whereas the Vickers hardness value of the 5 ton load is 522HV1.

At 1250 ˚C, the greatest value of hardness was achieved for 1 ton compaction load which had also the maximum sintered densification as well. The plot of hardness versus compaction load clearly shows the increasing trend of hardness values by the increase of compaction loads at lower sintering temperatures whereas at 1250 ˚C, where sintering is almost complete the highest value is achieved by the pellet compacted at 1 ton compaction load.

Table 5.5 Effect of compaction load on Vickers Hardness value

Compaction Load(ton)	HV1 at 850˚C	HV1 at 1050˚C	HV1 at 1250˚C
1	200	422	625
2	204	432	570
5	366	525	583

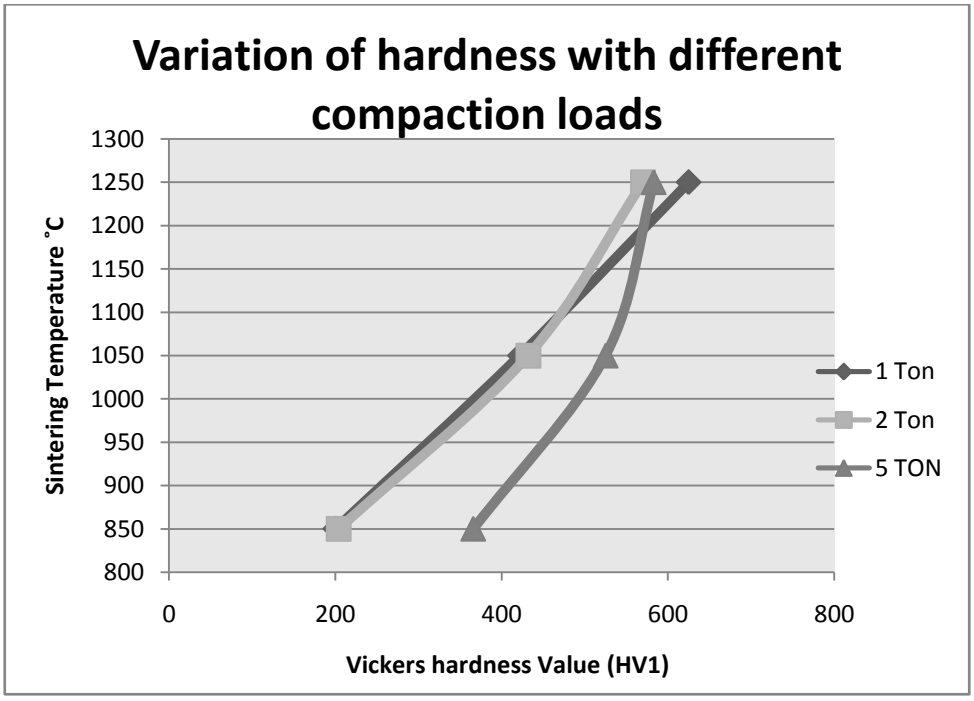

Figure 5.10 Effect of compaction load on Vickers Hardness value

5.4.2 Effect of Sintered density on Hardness value

The effect of sintered density on hardness values was studied and observed that sintered density has direct relationship with the hardness values.

The hardness values were found maximum for the pellets having the highest sintered densification and vice versa. It is clear from the data below that 625HV1 was achieved for the pellet having 98% sintered densification. Also the pellet having minimum sintered densification of 85% had the lowest hardness value of 200HV1.

Table 5.6 Effect of sintered density on Vickers Hardness value

Compaction Load(ton)	Sintered Density (850˚C)	HV1 at 850˚C	Sintered Density(1050˚C)	HV1 at 1050˚C	Sintered Density (1250˚C)	HV1 at 1250˚C
1	2.7	200	2.95	422	3.12	625
2	2.62	204	2.87	432	2.97	570
5	2.9	366	3.01	525	2.85	583

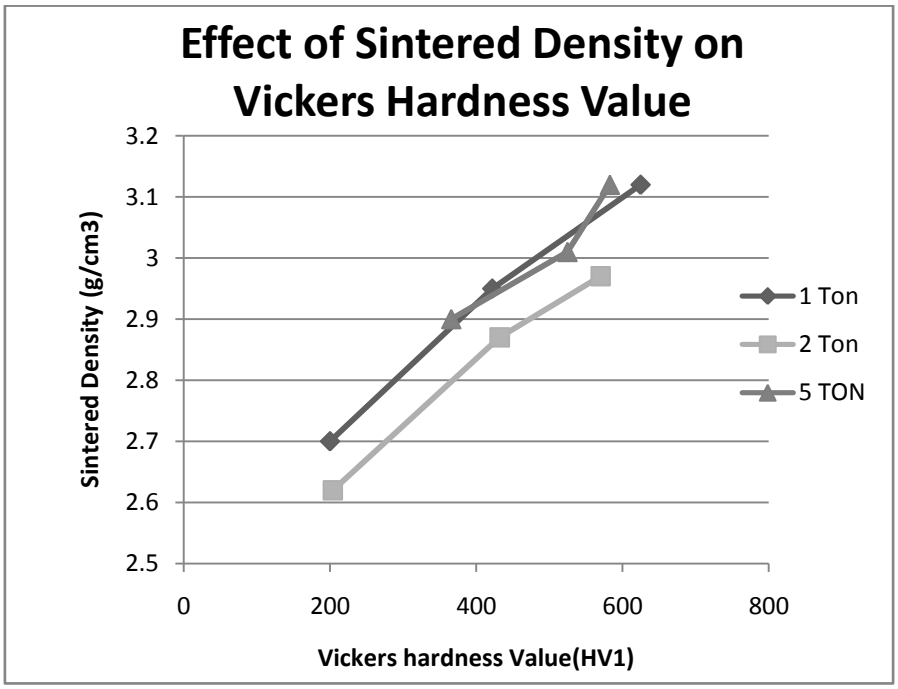

Figure 5.11 Effect of sintered density on Vickers Hardness value

5.4.3 Effect of Sintering temperature on Vickers hardness value

The sintering temperature has also the same effect as the sintered density. It was observed that at 850 ˚C the hardness values remained in the range of 200 to366 HV1 and it increased with the increase in sintering temperature. At 1050 ˚C the hardness value were in the range of 422 to 525HV1.

The hardness values reached a maximum value of 625HV1 at a sintering temperature of 1250 ˚C which had also maximum sintered densification of 98%.

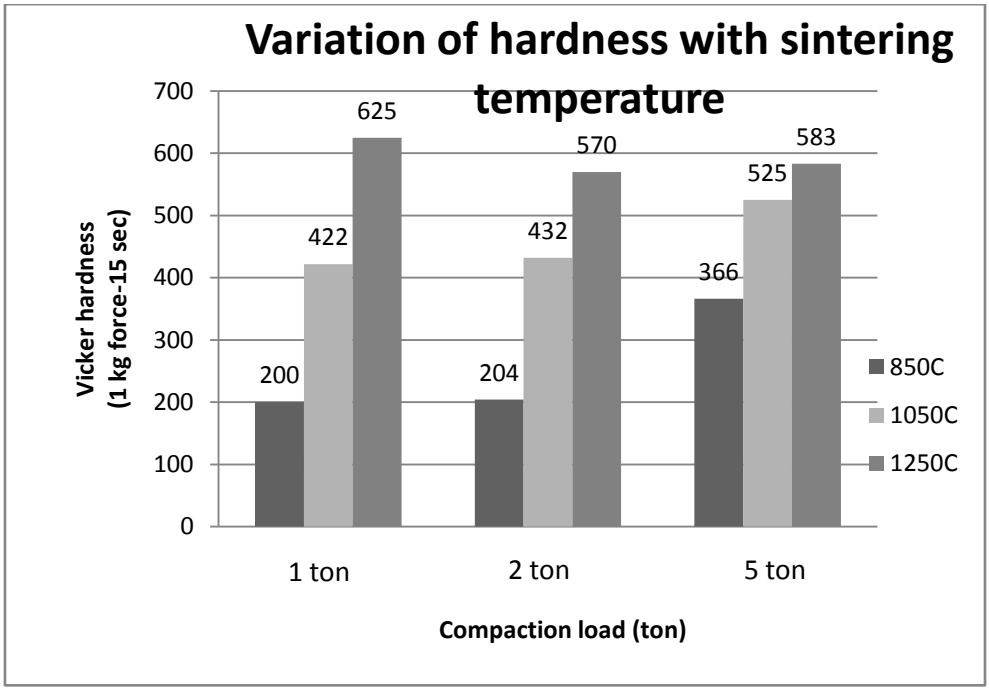

Figure 5.12 Effect of Sintering temperatures on Vickers hardness value

5.4.4 Effect of Sintering time on Vickers hardness value

The effect of sintering time on the resultant hardness values was also studied. The results clearly show that when the sintering time at the sintering temperature is decreased from 3 hours to 1 hour, the hardness values at lower temperatures are very much affected. At higher sintering temperature 1250 ˚C, the effect of decreasing sintering time on the hardness values was very little. This is because of the different sintering stages at these temperatures. At lower temperature 850 ˚C, the sintering is at its initial stage. So it needs much more time to achieve better results.

The data below shows that the hardness values at 850 ˚C decreased from 200HV1 to 45HV1 when the sintering time is decreased from 3 hours to 1 hour. The hardness values at 1050 ˚C are decreased from 422HV1 to 361 HV1 when the sintering time is decreased from 3 hours to 1 hour. This time there is little difference in the two values as sintering is in the intermediate stage and the effect of time is also decreased as compared to 850 ˚C values.

At the final stage of sintering at 1250 ˚C, the hardness values were studied by varying the time from 3 hours to 2 hour and 1 hour. It was found that the hardness decreased from 625HV1 to 570HV1 and 512HV1 respectively when the sintering time was decreased from 3 hours to 2 hour and 1 hour.

Table 5.7 Effect of Sintering time on Vickers hardness value

Sintering Temperature (°C)	Sintering Time (hours)	Vickers Hardness Value (HV1)
850	1	45
850	3	200
1050	1	361
1050	3	422
1250	1	512
1250	2	570
1250	3	625

5.5 Biaxial Flexural test

Biaxial flexural test was performed by taking the samples sintered at the three sintering temperatures which were compacted using 1 ton load. The test was performed by using ASTM standard F394-78 which is basically a ring-on-ring test. The speed of the testing was set to 1mm/min. The diameter and thickness of each sample varied and was calculated by screw gauge. Each sample was measured 5 times and an average value for diameter and thickness was taken. The pellet was polished on fine polishing cloth using 0.05 micron Alumina powder to make both the surfaces flat so that it does not affect the final results. The flexural strength was calculated by applying the load on the pellet which was placed in a die having dimensions as referred by the ASTM standard test geometry. The flexural strength values varied for each set of pellets although all were compacted and sintered at the same conditions. Poisson's ratio for HA was taken as 0.25.

Table 5.8 Flexural strength data

Sample code	Standard Deviation	Mean Flexural strength(MPa)
850-1	3.43	13.96
1050-1	4.48	24.76
1250-1	10.97	29.97

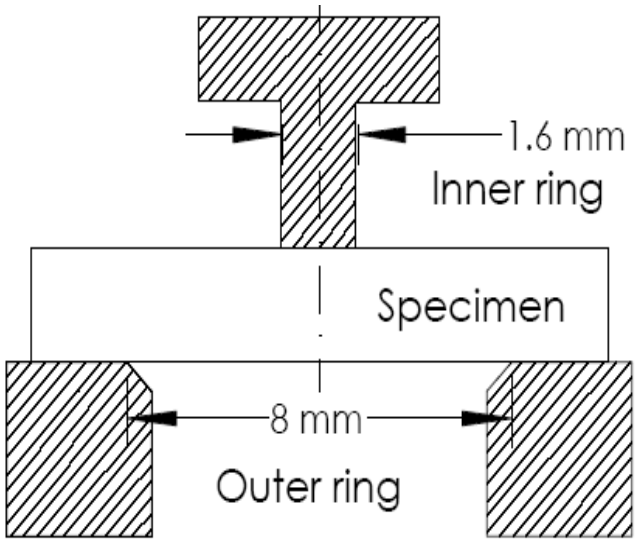

Figure 5.13 test geometry according to ASTM F394-78

$S = - 0.2387P(X – Y) / d2$

Where S is the flexure strength (MPa)

P total load causing fracture (N);

d the specimen thickness (mm);

Where,

$X = (1+\upsilon) \ln (B/C)^2 + [(1-\upsilon) /2] (B/C)^2$

$Y = (1+\upsilon) [1+ \ln (A/C)^2] + (1-\upsilon) (A/C)^2$

υ= Poisson's ratio;

A= radius of support circle (mm);

B = radius of loaded area or ram tip (mm);

& C = radius of specimen (mm).

A value of 0.25 was assumed for Poisson's ratio

Table 5.9 Biaxial flexural test data

Sample ID	D (Specimen thickness) (mm)	Sintered Density (g/cm^3)	Flexural Strength (MPa)
850-1	4.29	2.89	15.45
850-1	4.56	2.90	16.40
850-1	4.57	2.85	10.04
1050-1	4.95	2.95	12.43
1050-1	4.76	2.95	15.74
1050-1	4.15	2.95	21.00
1050-1	4.21	2.89	10.44
1050-1	4.45	2.95	19.43
1250-1	1.96	2.97	38.67
1250-1	1.83	2.85	31.47
1250-1	4.22	3.12	39.79
1250-1	4.31	3.08	25.34
1250-1	3.69	2.85	11.11
1250-1	4.47	3.02	18.49
1250-1	4.13	3.01	15.23
1250-1	4.42	3.05	16.84

5.5.1 Variation of Flexural strength with temperature

The effect of sintering temperature on flexural strength was studied and it was observed that with the increase of Sintering temperature the mechanical properties are improved. The pellets sintered at 850˚C had the lowest flexural strength in the range of 10-16MPa as these pellets had the lowest Sintered density.

The flexural strength of the pellets sintered at 1050˚C improved and an average of 25MPa was obtained which was better than before.

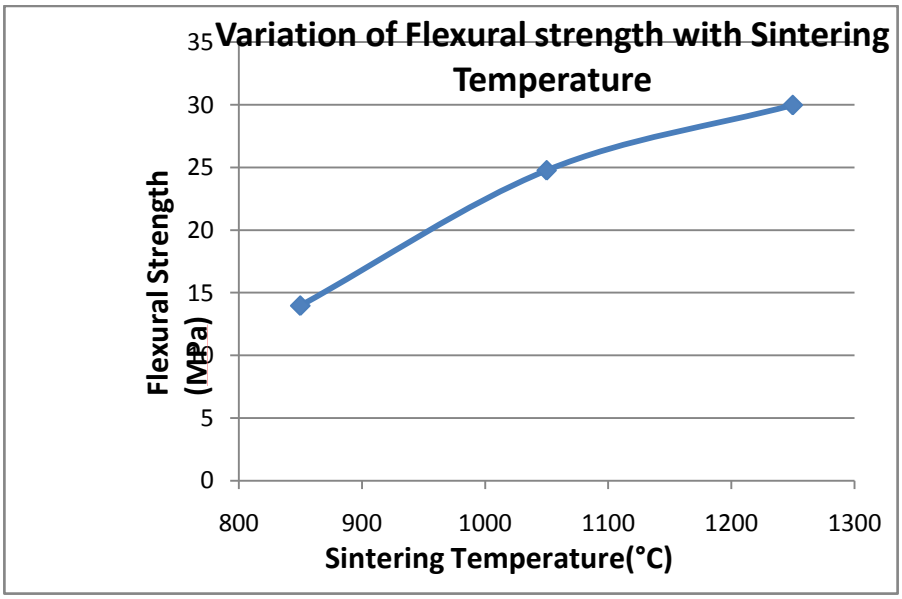

Figure 5.14; Variation of Flexural strength with sintering temperature

Similarly the pellets sintered at 1250 ˚C achieved the maximum strength of 40MPa. These pellets also had the maximum sintered densification of 98%. It is clear from the data obtained that flexural strength increases with the increase in sintered density which increases with the increase of sintering temperature up to 1250 ˚C. Above 1250 ˚C it may be supposed that some changes may occur in these properties due to the decomposition of HA in other phases.

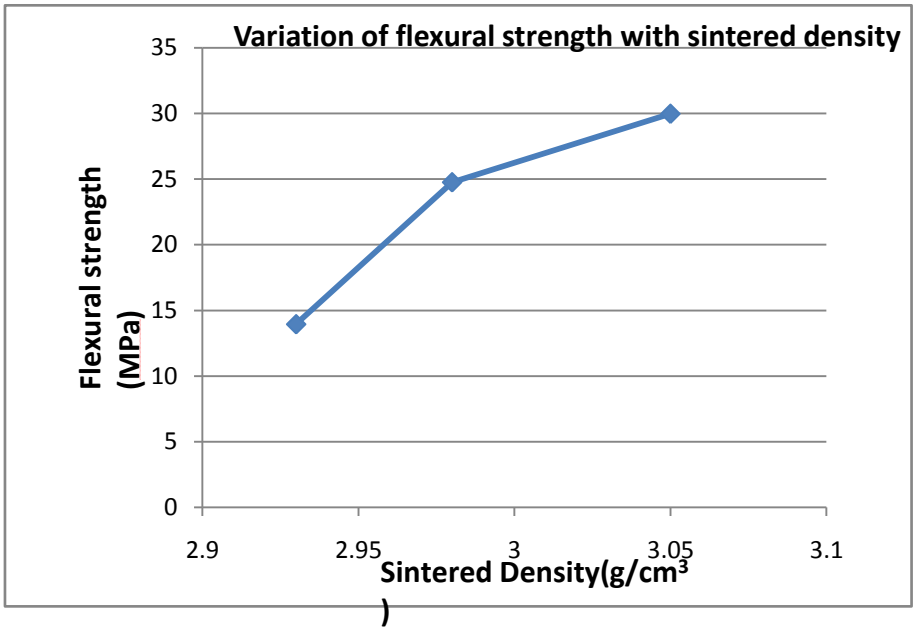

Figure 5.15; Variation of Flexural strength with sintered density

5.6 To study the Phase stability of HA using XRD

The phase stability of HA was studied by using XRD analysis. The pellets sintered at different sintering temperatures were analyzed by using XRD. All Diffraction peaks could be perfectly indexed to hexagonal HA with lattice constants a= 9.42Å and c= 6.879Å (JCPDS card No. 00-074-0565). The results apparently indicate that the pellets consist of hydroxyapatite phase with no or insignificant amount of impurities.

The crystallite size of the sintered HA pellets is calculated by the Scherer's Formula [1] as follows

$$t = \frac{0.9\lambda}{\beta\cos\theta}$$

Where t is the crystallite size of the as received HA, λ is the wavelength of Cu Kα radiation (1.54Å), β is the intensity of peaks at full width half maximum (FWHM) and θ is the Bragg's angle.

The average crystallite size as calculated by this formula is tabulated below. No other phases such as α-TCP and β-TCP were observed confirming the phase purity of HA.

Table 5.10 Crystallite size of sintered HA

	Un-sintered HA	850˚C	1050˚C	1250˚C
Crystallite Size	15 nm	54 nm	73 nm	95nm

The crystallite size increased with sintering temperature. Initially the crystallite size of un-sintered HA powder was 15nm which then gradually increased to 54nm, 73nm and 95nm respectively for 850˚C, 1050˚C and 1250˚C.

The samples sintered at 850˚C, 1050˚C and 1250˚C were then analyzed by XRD in order to check the phase stability of HA and the patterns obtained from XRD were matched with the standard pattern of HA. Figure below shows the indexed patterns of HA sintered as well as un-sintered HA. No new peaks were identified confirming the phase stability of HA. Even at 1250˚C the HA phase was pure.

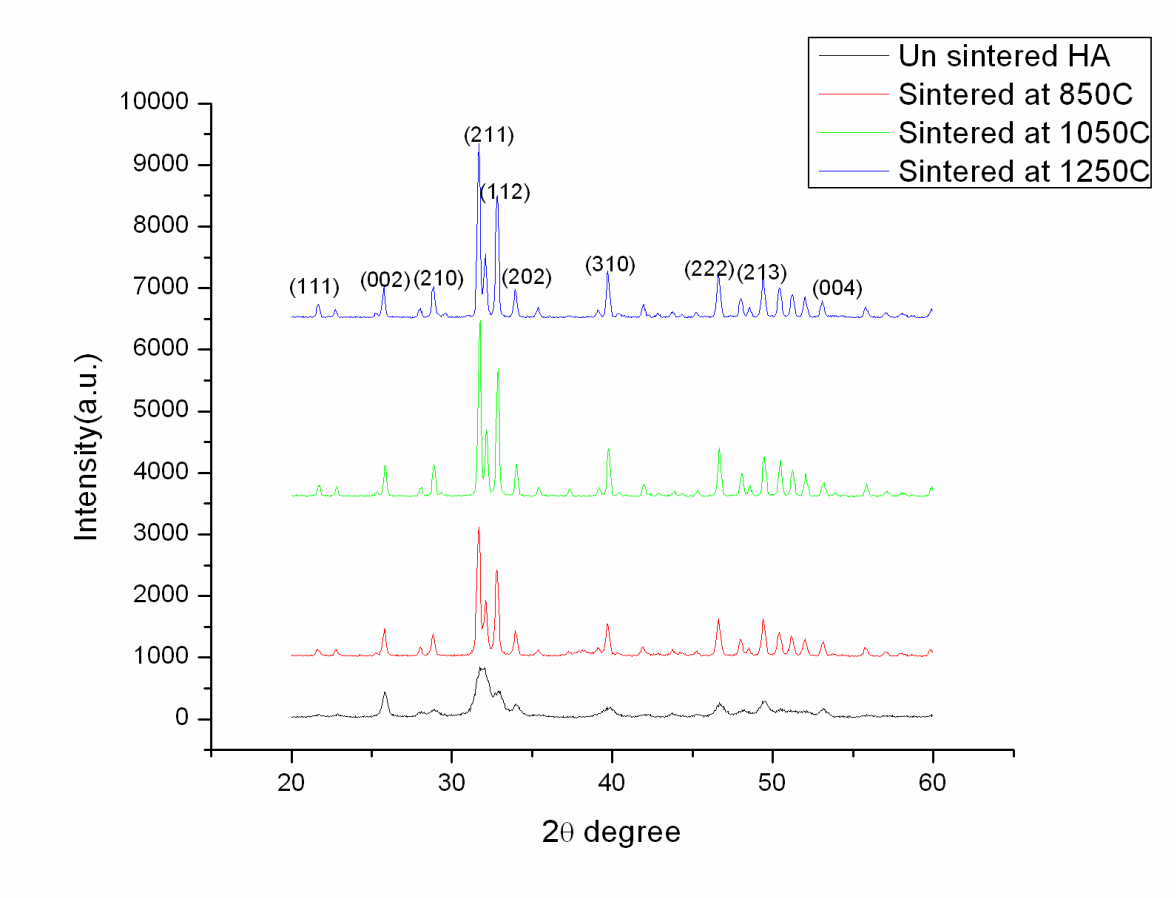

Figure 5.16 XRD Patterns of pure Hydroxyapatite

5.7 Effect of Sintering Variables on Grain growth

The effect of sintering time and sintering temperature on the resultant grain growth was studied by using SEM.

5.7.1 Effect of sintering temperature on Grain growth

Hydroxyapatite was sintered at three temperatures 850˚C, 1050˚C and 1250˚C. As the temperature was increased, sintering started and it was observed in the SEM that with increasing sintering temperature the grain size grows. Most probably the larger grains grow on the expense of smaller grains. The grain size was calculated by Lineal Intercept Method and averages of 200 grains were measured for each sample. Different areas were selected during SEM so that actual size can be measured.

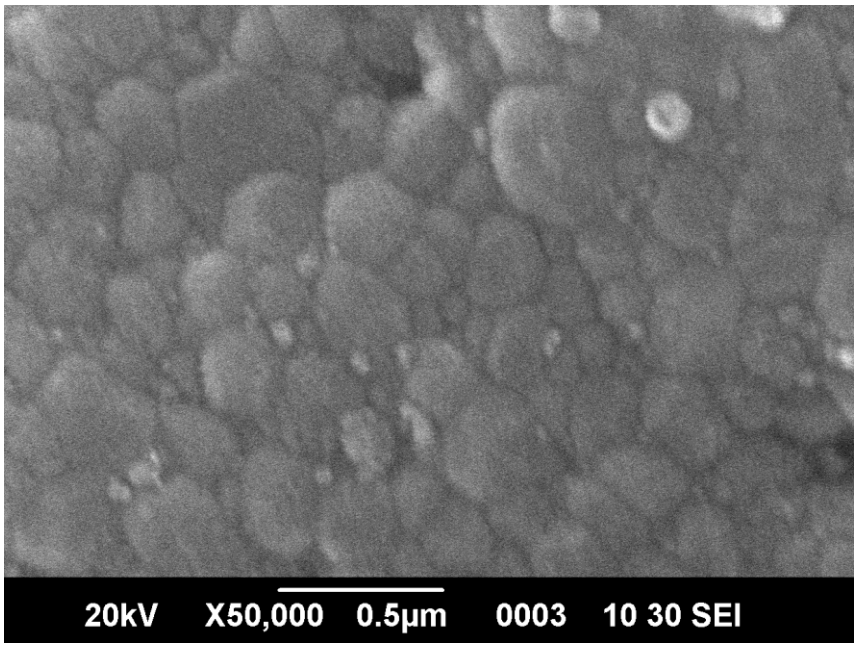

Figure 5.17 SEM micrograph of HA sintered at 850˚C

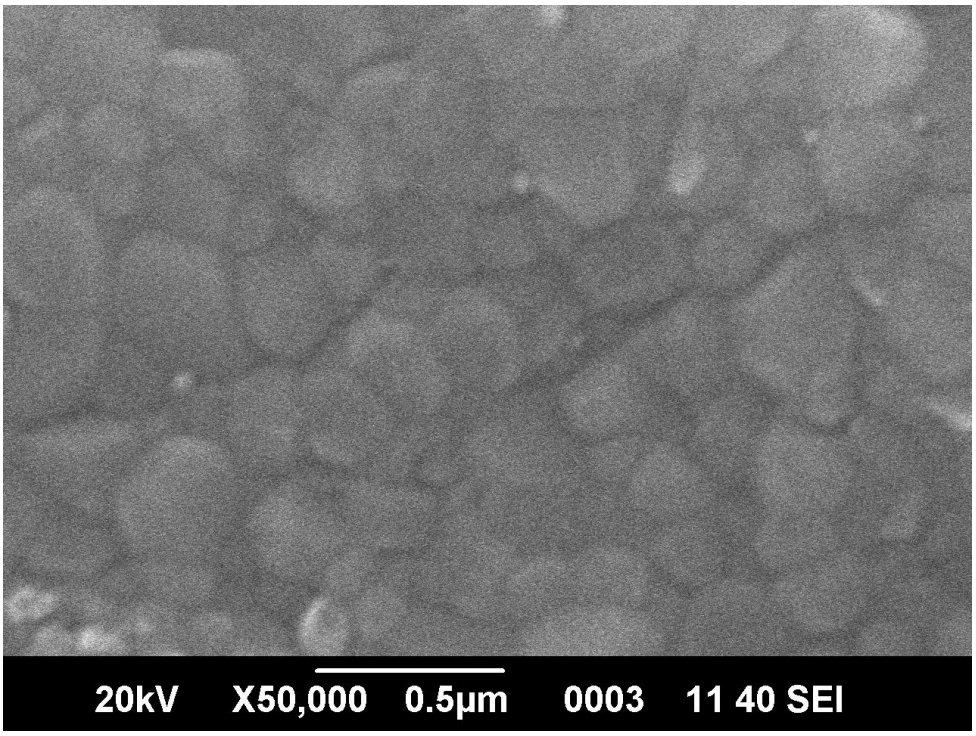

Figure 5.18 SEM micrograph of HA sintered at 1050˚C

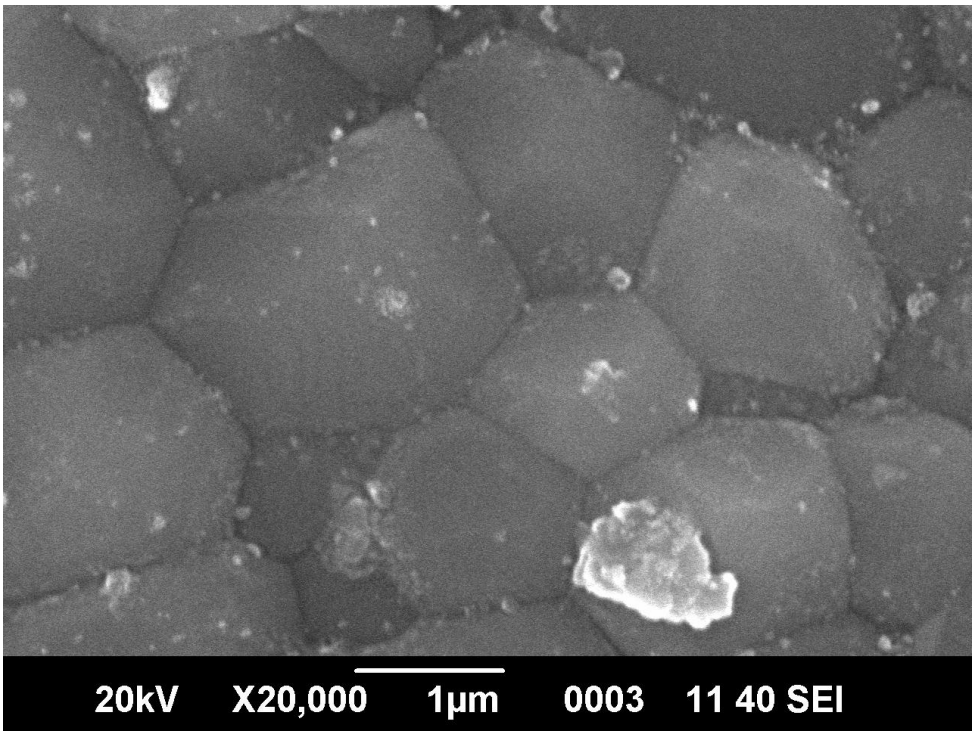

Figure 5.19 SEM micrograph of HA sintered at 1250˚C

5.7.2 Effect of sintering time on Grain growth

The sintering time/soaking time was also varied to study the behavior of grain growth and it was observed that the grain size was decreased to 1.15µm from 1.82µm when the sintering time was reduced from 3 hours to 1 hour. The grain size increased from 1.15µm to 1.60µm when the sintering time was increased from 1 hour to 2 hours. The SEM micrographs clearly show the grain growth during sintering.

Table 5.11 Average grain size calculation of Sintered HA

Sintering Temperature ˚C	Sintering time (hours)	Average Grain size
850˚C	3	0.22µm
1050˚C	3	0.30µm
1250˚C	3	1.82µm
1250˚C	2	1.60µm
1250˚C	1	1.15µm

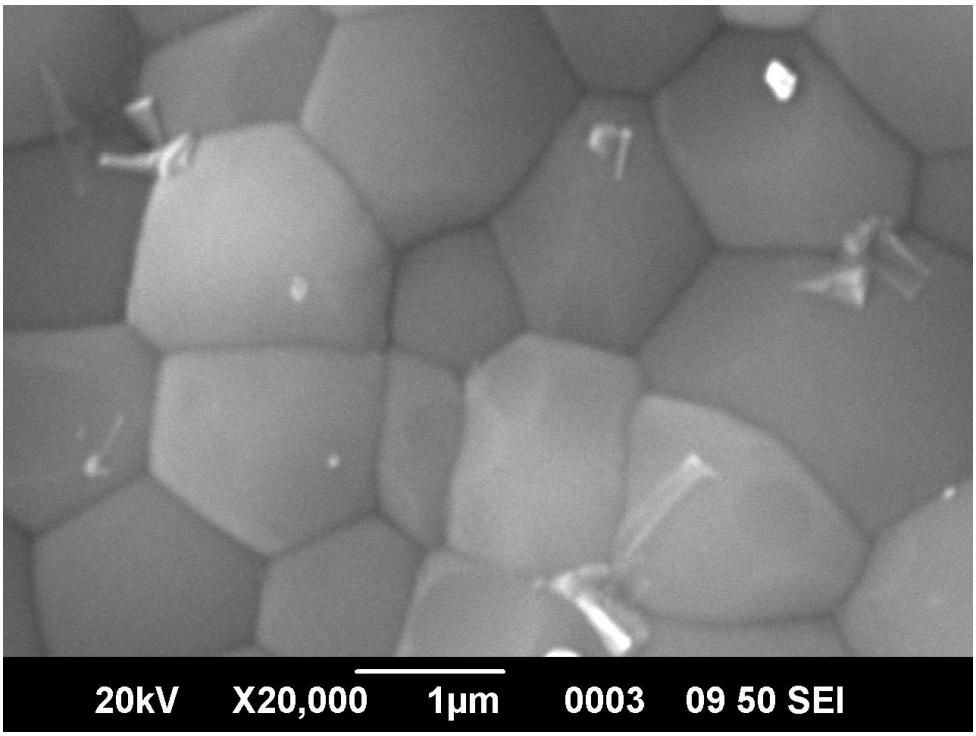

Figure 5.20 SEM micrograph of HA sintered at 1250˚C for 1 hour

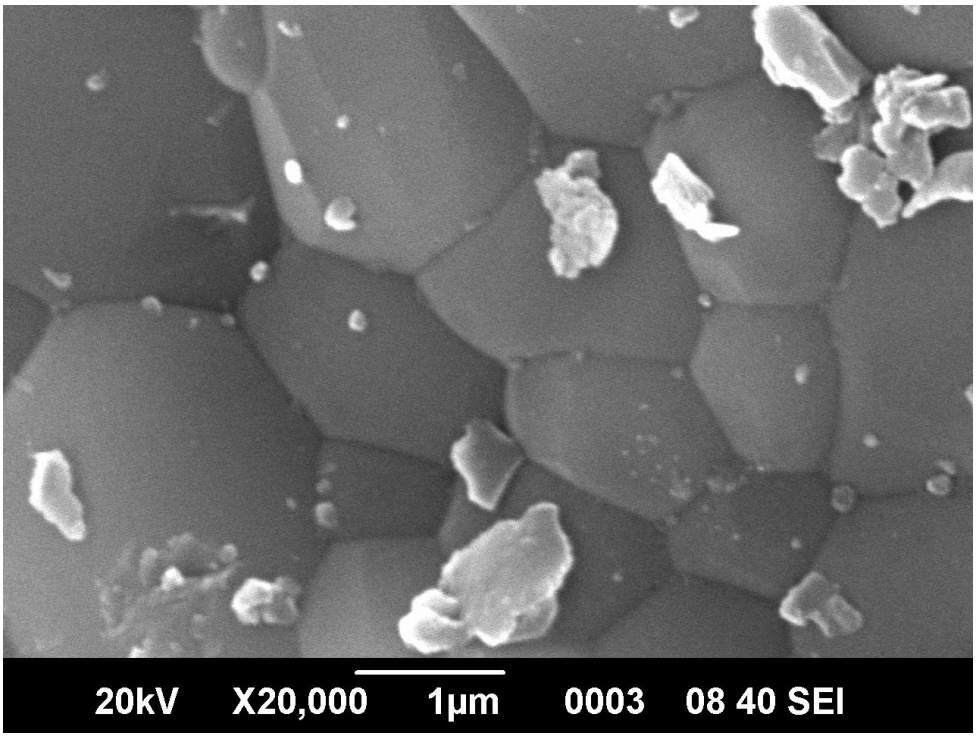

Figure 5.20 SEM micrograph of HA sintered at 1250˚C for 2 hours

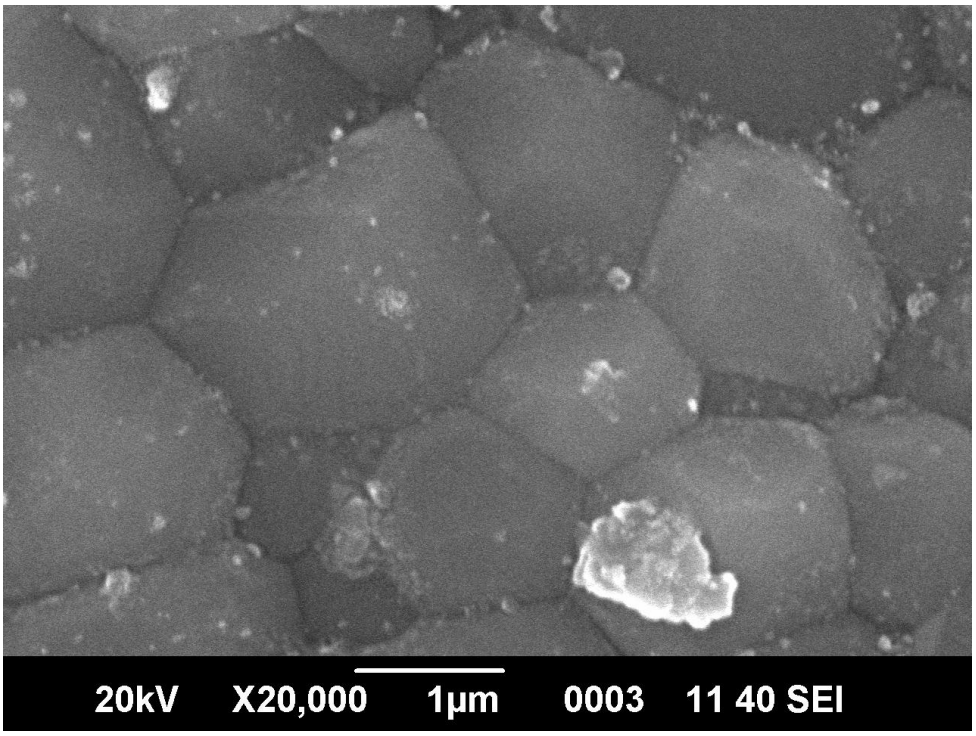

Figure 5.21 SEM micrograph of HA sintered at 1250˚C for 3 hours

CHAPTER 6

CONCLUSION & FUTUREWORK

6.1 Conclusion

- Optimum compaction load
  - Green density maximum 50% for 5 ton compaction load
- Best sintering conditions
  - Pellets were sintered to a relative density of 98% theoretical density at a temperature of 1250^0 C and compaction load 1 ton
    - Maximum average Vickers Hardness 625 (+28) HV1
    - Maximum flexural strength 40(+10) MPa
- XRD analyses
  - No α TCP and β TCP were observed
  - No significant phase changes even at a temperature of 1250^0 C.
- At higher compaction load of 5 ton,
  - we can achieve a relative sintered density of 95% even at 1050^0 C.
- By using Nano crystalline HA,
  - Relative sintered density of 90% even at very low sintering temperature of 850^0 C at 5 ton compaction load.
- By the decrease of soaking time from 3 hours to 1 hour :
  - Sintered density at 850^0 C ---85% to 50% whereas at higher temperatures the decrease in density was only 4 to 6%.

- Grain size measurement
  - At 1250^0C decreased from 1.82μm to 1.15μm by varying the soaking time from 3 hours to 1 hour

6.2 Future Work

Following future work needs to be done for improvement and further development of present results.

6.2.1 Use of Sintering Additives

The use of sintering additives such as Calcium oxide (CaO) and Sodium Phosphate ($Na_3(PO_4)_2$ 12 H_2O) can be used to enhance densification of pure HA. As the melting point of sodium phosphate is 1583°C so solid state sintering can be done easily whereas for low melting compounds such as Sodium Carbonate Na_2CO_3 (Melting Point 851°C) can also be used in which the sintering additive melts and better sintering takes place.

6.2.2 Use of other Sintering Processes

Another parameter to control the mechanical properties of HAis the final grain size of near full dense samples [2].The conventional sintering (CS) method is generallyincapable of preparing full dense ultra-fine grained ceramics. Thefact is that the grain growth and densification are both driven bydiffusive mechanisms which result to the simultaneous activationof densification and grain growth in the later stage of sintering[3]. Spark plasma sintering (SPS) [4,5] and hot pressing [6] arealso, two promising techniques for production of nanostructuredceramics. Guo et al. [5], have, for instance, spark plasma sinteredsynthesized HA nanopowders at a low temperature (825 ◦C) andshort time (3 min), while the final grain size became <130±44 nm.Using SPS equipment, Kumar et al. [1] managed to improve thefracture toughness of HA specimens from 0.77 (conventionally sintered)to 1.17MPam1/2 (spark plasma sintered).

Compositesof HAwith other ceramics such as Alumina, Zirconia can be tried to enhance mechanical properties.

References:

[1] R. Kumar, K.H. Prakash, P. Cheang, K.A. Khor,2005 Acta Materialia‘53 2327–2332.

[2] S. Ramesh, C.Y. Tan, I. Sopyan, M. Hamdi,W.D. Teng,W.D. Teng, (2007) Advanced Materials8 124–130.

[3] M. Mazaheri, A.M. Zahedi, S.K. Sadrnezhaad, (2008) Journal of the American CeramicSociety 91 56–63.

[4] Y.W. Gu, N.H. Loh, K.A. Khor, S.B. Tor, P. Cheang,(2002) Biomaterials 23 37–43.

[5] X. Guo, P. Xiao, J. Liu, Z. Shen,(2005) Journal of the American Ceramic Society 88 1026–1029.

[6] A.Weibel, R. Bouchet, R. Denoyel, P. Knauth, (2007) Journal of European Ceramic Society 27 2641–2646.